

## A New Approach to Divergence Cleaning in Magnetohydrodynamic Simulations

Andreas Dedner\* and Matthias Wesenberg

*Institut für Angewandte Mathematik, Universität Freiburg, Freiburg, Germany*

For the simulation of electrically conducting fluid flow the equations of magnetohydrodynamics (MHD) have to be solved. These combine the Euler equations of gas dynamics and the Maxwell equations. They are a system of nonlinear conservation laws for the fluid density  $\rho$ , momentum  $\rho\mathbf{u}$ , magnetic field  $\mathbf{B} = (B_x, B_y, B_z)^T$ , and total energy density  $e$ .  $\mathbf{u} = (u_x, u_y, u_z)^T$  denotes the fluid velocity. Ignoring higher order effects like viscosity and resistivity we obtain the system

$$\partial_t \rho + \nabla \cdot (\rho \mathbf{u}) = 0, \quad (1a)$$

$$\partial_t (\rho \mathbf{u}) + \nabla \cdot \left[ \rho \mathbf{u} \mathbf{u}^T + \left( p + \frac{1}{2} |\mathbf{B}|^2 \right) \mathcal{I} - \mathbf{B} \mathbf{B}^T \right] = 0, \quad (1b)$$

$$\partial_t \mathbf{B} + \nabla \cdot (\mathbf{u} \mathbf{B}^T - \mathbf{B} \mathbf{u}^T) = 0, \quad (1c)$$

$$\partial_t e + \nabla \cdot \left[ \left( e + p + \frac{1}{2} |\mathbf{B}|^2 \right) \mathbf{u} - \mathbf{B} (\mathbf{u} \cdot \mathbf{B}) \right] = 0. \quad (1d)$$

The additional constraint

$$\nabla \cdot \mathbf{B} = 0 \quad (1e)$$

ensures a divergence-free magnetic field. This system has to be closed by an equation of state for the fluid pressure  $p$ . For the work presented here we assume a perfect fluid so that  $p = (\gamma - 1) \rho \varepsilon$  with a constant adiabatic exponent  $\gamma > 1$ . The internal energy  $\varepsilon$  is given by  $\varepsilon = \frac{e}{\rho} - \frac{1}{2} |\mathbf{u}|^2 - \frac{1}{2\rho} |\mathbf{B}|^2$ . The scheme presented in our talk can be also used for more complex pressure laws.

For the conservative quantities  $\mathbf{U} = (\rho, \rho \mathbf{u}, \mathbf{B}, e)^T$  we have to prescribe suitable initial and boundary conditions. In particular the constraint (1e) requires that the initial data for the magnetic field has zero divergence. Equation (1c) can be rewritten in the equivalent form  $\partial_t \mathbf{B} + \nabla \times (\mathbf{B} \times \mathbf{u}) = 0$ . Since the divergence of a curl vanishes identically the divergence of the magnetic field will stay zero for all time if it is zero initially. Hence numerical methods are usually based only on the hyperbolic evolution equations (1a) — (1d).

In simulations divergence errors can be introduced by approximation errors if the divergence constraint (1e) is not explicitly taken into account. These errors can then increase with time and will result in unphysical solutions: Magnetic field lines can have wrong topologies leading to plasma transport *orthogonal* to the magnetic field. This effect is discussed among others by Brackbill and Barnes [BB80]. Even if the overall solution is not strongly affected by local divergence errors, they generally cause severe problems for the stability of the scheme.

In our numerical scheme we use a standard finite-volume approach with approximate Riemann solvers for the computation of the flux functions across cell interfaces [DRW99, DKRW01]. This requires an approximate solution of (1a) — (1d) in one space dimension. In 1d the evolution equation for the normal magnetic field  $B_x$  (1c) and the divergence constraint (1e) read

$$\partial_t B_x = 0 \quad \text{and} \quad \partial_x B_x = 0. \quad (2)$$

Therefore  $B_x$  may vary neither in space nor time. On the other hand the normal magnetic field component are in general discontinuous across a cell interface. Thus the value of  $B_x$  which we use for the solution of the one-dimensional Riemann problem is not constant as required by (2). This leads to unphysical numerical fluxes and the loss of stability in the two- and three-dimensional schemes.

In [DKK<sup>+</sup>02] we extend a correction method developed for the Maxwell equations in [MOS<sup>+</sup>00]. This method is based on a modified equation for the magnetic field and introduces a new unknown function  $\psi$ . The new equation for the magnetic field which replaces (1c) and the equation for the auxiliary function  $\psi$  are given by

$$\partial_t \mathbf{B} + \nabla \cdot (\mathbf{u} \mathbf{B}^T - \mathbf{B} \mathbf{u}^T) + \nabla \psi = 0, \quad (3)$$

$$\mathcal{D}(\psi) + \nabla \cdot \mathbf{B} = 0, \quad (4)$$

where  $\mathcal{D}$  is a linear differential operator. The modified system is called the *generalized Lagrange multiplier* (GLM) formulation of the MHD equations. In [MOS<sup>+</sup>00] different choices for  $\mathcal{D}$  were suggested which result in an *elliptic*, a *parabolic* or a *hyperbolic* correction. We show in numerical tests that the best choice is to combine the damping effect of the parabolic approach and the advection within the hyperbolic approach. This can be achieved by choosing  $\mathcal{D}(\psi) := \frac{1}{c_h^2} \partial_t \psi + \frac{1}{c_p^2} \psi$  with two constants  $c_h > 0, c_p > 0$ . By combining equations (4) and (3) we arrive at the telegraph equation for the divergence of the magnetic field  $\partial_{tt}^2(\nabla \cdot \mathbf{B}) + \frac{c_h^2}{c_p^2} \partial_t(\nabla \cdot \mathbf{B}) - c_h^2 \Delta(\nabla \cdot \mathbf{B}) = 0$ .

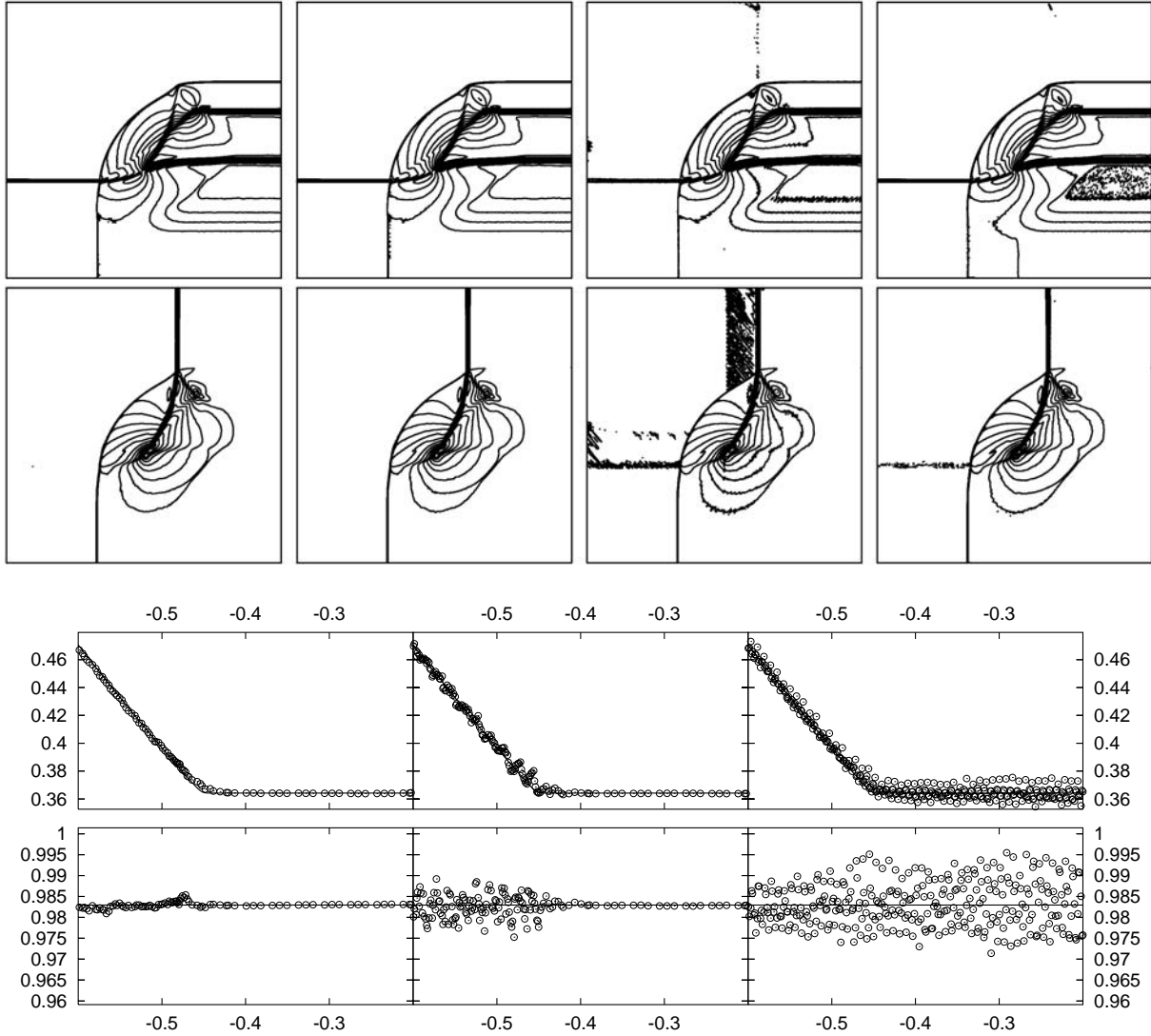


Figure 1: A two-dimensional Riemann problem computed on  $[-1, 1] \times [-1, 1]$  using a second order finite-volume scheme. We show  $B_x$  and  $B_y$ . The two top rows show (from left to right) the mixed approach, the hyperbolic approach, no correction and the source term technique. The two bottom rows show the solutions along the ray at  $x = 0.92$ , using the mixed GLM method, no correction and the source term approach. Note that in this case  $B_y$  should be a constant value.

For all choices of  $\mathcal{D}$  the GLM-MHD system (1a), (1b), (3), (1d), and (4) is hyperbolic and the equations for the physical quantities  $\rho, \rho \mathbf{u}, \mathbf{B}$ , and  $e$  remain in conservation form. We also demonstrate in [DKK<sup>+</sup>02] that for the one-dimensional setting divergence errors in the initial data are damped in the parabolic approach and transported out of the domain in the hyperbolic approach. We will also study the mixed approach in the one-dimensional case.

The elliptic approach is equivalent to the well known projection scheme and therefore requires solving a Laplace equation. The parabolic approach requires taking into account a second-order term in divergence form in the induction equation and can be

added in the finite-volume framework. The hyperbolic and the mixed approach lead to a simple modification of the numerical flux. The additional cost can be reduced to solving a linear two by two system for  $\psi$  and the normal component of the magnetic field.

In addition to the results published in [DKK<sup>+</sup>02] our talk includes a comparison of the parabolic and elliptic approach with the hyperbolic and mixed correction. As reference technique we use the source term approach developed by Powell and others [BB80, Pow94]. For most test cases we found that the mixed hyperbolic / parabolic approach is superior compared to the other methods tested as shown in Fig. 1. We found that our approach leads to very stable numerical schemes for solving the MHD equations in two and three space dimensions.

## Acknowledgments

The authors were supported by the DFG priority research program “Analysis and Numerics for Conservation Laws” (ANumE). We present joint work with the authors of [DKK<sup>+</sup>02].

## References

- [BB80] J.U. Brackbill and D.C. Barnes, *Note: The effect of nonzero  $\nabla \cdot \mathbf{B}$  on the numerical solution of the magnetohydrodynamic equations*, J. Comput. Phys. **35** (1980), 426–430.
- [DKK<sup>+</sup>02] A. Dedner, F. Kemm, D. Kröner, C.-D. Munz, T. Schnitzer, and M. Wesenberg, *Hyperbolic divergence cleaning for the MHD equations*, J. Comput. Phys. **175** (2002), no. 2, 645–673, doi:10.1006/jcph.2001.6961.
- [DKRW01] A. Dedner, D. Kröner, C. Rohde, and M. Wesenberg, *Godunov-type schemes for the MHD equations*, Godunov Methods: Theory and Applications (E.F. Toro, ed.), Kluwer Academic/Plenum Publishers, November 2001, pp. 209–216.
- [DRW99] A. Dedner, C. Rohde, and M. Wesenberg, *A MHD-simulation in solar physics*, Finite Volumes for Complex Applications II: Problems and Perspectives (Paris) (R. Vilsmeier, F. Benkhaldoun, and D. Hänel, eds.), Hermès Science Publications, 1999, pp. 491–498.
- [MOS<sup>+</sup>00] C.-D. Munz, P. Omnes, R. Schneider, E. Sonnendrücker, and U. Voss, *Divergence correction techniques for maxwell solvers based on a hyperbolic model*, J. Comput. Phys. **161** (2000), no. 2, 484–511.
- [Pow94] K.G. Powell, *An approximate Riemann solver for magnetohydrodynamics (that works in more than one dimension)*, ICASE-Report 94-24 (NASA CR-194902), NASA Langley Research Center, Hampton, VA 23681-0001, 8. April 1994.

### Discontinuous solutions of Hamilton-Jacobi equations: existence, uniqueness and regularity

Bo Su

*University of Wisconsin-Madison*

In this talk, we address basic questions of the discontinuous solutions of Hamilton-Jacobi equations: existence, uniqueness, and regularity. The existence of  $L^\infty$  solutions is proven for general Hamiltonians. Then we clarify the connections between the existing notions including the classical semicontinuous solutions by Ishii. We prove the uniqueness in the measure sense of discontinuous solutions including the classical semicontinuous solutions,  $L^\infty$  solutions for the important special class of Hamiltonians-convex Hamiltonians. They are the same in the measure sense. The regularity after finite time property, a new genuinely nonlinear phenomenon, of Hamilton-Jacobi equations for locally strictly convex Hamiltonians  $H = H(p)$  such as

$H(p) = (1 + |Du|^2)^{\frac{1}{2}}$  is established. That is, with discontinuous initial data, the discontinuous solutions of  $u_t + H(Du) = 0$  becomes Lipschitz continuous in finite time. The difference between regularity of solutions of the typical strictly convex Hamilton-Jacobi equations  $u_t + |Du|^2 = 0$  and the typical locally strictly convex Hamilton-Jacobi equations  $u_t + (1 + |Du|^2)^{\frac{1}{2}} = 0$  is similar to that between the solutions of the typical uniform parabolic equation  $u_t - \Delta u = 0$  and the typical degenerate parabolic equation  $u_t - \Delta u^2 = 0$ .

## 4.5 Monday, Session 3 (morning): Viscous conservation laws I

### On the Boundary Control of Systems of Conservation Laws

Giuseppe Maria Coclite\* and Alberto Bressan

*S.I.S.S.A., Via Beirut 4, Trieste 34014 Italy*

In this paper we study the problem of the boundary controllability for a  $n \times n$  systems of conservation laws on a bounded interval

$$u_t + f(u)_x = 0, \quad t \geq 0, \quad x \in ]a, b[. \quad (1)$$

We study the property of the attainable set  $\mathcal{R}(T)$  (i.e. the set of the maps  $\varphi \in L^1([a, b])$  such that  $u = u(t, x)$  is an entropic solution (1) such that  $u(T, \cdot) = \varphi$ ). We assume that (1) is strictly hyperbolic, satisfying the Lax admissibility conditions and  $Df$  has eigenvalue bounded away from zero (i. e. the boundaries are not characteristic). We prove two results.

I) Given a constant state  $u^*$  constant and an initial data  $\bar{u} \in BV([a, b])$  with small total variation and close to  $u^*$  in  $L^1$  norm, we prove the existence of a solution  $u = u(t, x)$  of (1) such that

$$u(0, \cdot) = \bar{u}, \quad \text{Tot. Var.} \{u(t)\} \leq C e^{-2\kappa t},$$

$$\int_a^b |u(t, x) - u^*| dx \leq C e^{-2\kappa t},$$

for some constants  $\kappa, C > 0$ . This provides the asymptotic controllability around a constant state.

II) We show with a counterexample that in general the constant states are not exactly attainable in finite time. We consider a  $2 \times 2$  system such that

$$r_1 \wedge r_2 < 0, \quad r_1 \wedge (Dr_1 \cdot r_1) < 0, \quad r_2 \wedge (Dr_2 \cdot r_2) < 0,$$

where  $r_1$  and  $r_2$  are the right eigenvectors of  $Df$ . The geometry of the system implies that the interactions between two shocks of the same family generates a shock in the other one and the one between a shock and a rarefaction generates rarefaction. Then the set of the maps with finitely many jumps, that generate shocks (and no rarefactions), and whose components (in Riemann coordinates) are piecewise increasing, is invariant. These remarks permit to show that if the set of the shocks of a solution is dense at the time  $t = 0$  then it is dense for each time  $t > 0$ .

### Stability Analysis for periodic solution waves in viscous conservation laws

Myunghyun Oh

*Ohio State University*

Nonclassical viscous conservation laws arising in multiphase fluid and solid mechanics exhibit a rich variety of traveling wave phenomena, including homoclinic (pulse-type) and periodic solutions along with the standard heteroclinic (shock, or front-type) solutions. Here, we investigate stability of periodic traveling waves within the abstract Evans function framework established by R.A. Gardner. Certain interesting oscillatory behavior detected by Frid-Liu and Čanić-Peters seems possibly related to the periodic waves. The obvious conjecture, by analogy with pattern formation in reaction-diffusion equations, would be that these represent stable periodic solutions, or fronts connecting such a stable solution to further (possibly unstable) periodic solutions. On the other hand, an alternative explanation was offered by Azevedo, Marchesin, Plohr, and Zumbrun involving metastable collections of slowly interacting shocks. Numerically observed patterns are well matched by patterns of either type.

Our main result divide into three separate parts, generalizing each of the three major directions that have been pursued in the viscous shock front case. The first result is to derive a useful *stability index* analogous to that developed by Gardner and

Zumbrun in the traveling front/pulse context, giving necessary conditions for stability with respect to initial perturbations that are periodic on the same period  $T$  as the traveling wave; moreover, we show that the periodic stability index has an interpretation analogous to that of the traveling front/pulse index in terms of well-posedness of an associated inviscid Riemann problem, now to be interpreted in a wider class of measure-valued solutions. A closely related calculation yields also a complementary *long-wave stability criterion* necessary for stability with respect to periodic perturbations of arbitrarily large period  $NT$ ,  $N \rightarrow \infty$ .

The stability index and long-wave stability criterion are explicitly evaluable in the same planar, Hamiltonian cases as is the index of Gardner–Zumbrun, and together yield rigorous results of instability similar to those obtained previously for pulse-type solutions; this is established through a novel *dichotomy* asserting that the two criteria are in certain cases logically exclusive. In particular, we obtain results bearing on the nature/formation of highly oscillatory Turing-like patterns observed numerically by Frid–Liu and Čanić–Peters in models of multiphase flow. Specifically, for the van der Waals model considered by Frid–Liu, we show instability of all periodic waves such that period increases with amplitude in the one-parameter family of nearby periodic orbits, and in particular of large- and small-amplitude waves; likewise, for a quadratic flux model like that considered by Čanić–Peters, we show instability of large-amplitude waves of the type lying near observed patterns, and of all small-amplitude waves.

The second result, generalizing the work of Zumbrun and Howard in the traveling pulse/front setting, is to establish sharp pointwise bounds on the Green’s function of the linearized evolution equations, provided that there holds an appropriate *Evans function condition* on the linearized operator about the wave, in this case equivalent to a spectral stability criterion introduced by Schneider in the context of periodic reaction–diffusion waves. An immediate consequence is that *strong spectral stability* (in the sense of Schneider) *implies linearized  $L^1 \rightarrow L^p$  asymptotic stability*, for all  $p > 1$ . On the other hand, we show that the strict version of Schneider’s condition generically fails in the conservation law setting, leading to complicated new “metastable” behavior reminiscent of that seen for degenerate, neutrally stable families in the traveling front/pulse case. Our results apply also to the reaction–diffusion setting, sharpening (at the linearized level) results obtained by Schneider using weighted norm/Bloch decomposition methods.

As in the traveling front case, the basic approach is to mimic in the Laplace transform setting the elementary Fourier-transform analysis of the constant coefficient case. However, the technical issues involved are rather different in the two cases. Somewhat surprisingly, we find the analogy to the constant-coefficient case to be rather stronger in the periodic coefficient case, permitting a more standard approach involving the explicit construction of “continuous” spectral measure as in the self-adjoint case. This is equivalent to the method of Zumbrun and Howard in this special case.

The third result is to derive a numerical test of periodic wave stability. We give numerical evidence that intermediate-amplitude waves are unstable as well. These results give support for an alternative mechanism of pattern formation conjectured by Azevedo, Marchesin, Plohr, and Zumbrun, not involving periodic waves. We show instability of all periodic waves in some example systems studied by Frid–Liu and Čanić–Peters. Together, the first and third has the implication that the oscillatory patterns they observed are formed by a mechanism substantially different from that of the reaction diffusion/pattern formation setting. The precise mechanism is still in question.

## 4.6 Monday, Session 3 (afternoon): Adaptive methods I

### Adaptive Mesh Redistribution Methods for Nonlinear Hamilton-Jacobian Equations

Tao Tang\*

*Dept of Mathematics, Hong Kong Baptist Univ., Hong Kong*

Hua-Zhong Tang

*School of Mathematical Sciences, Peking Univ, China*

Adaptive mesh redistribution (AMR) methods have important applications for a variety of physical and engineering areas. In the past two decades, there have seen many important progress in moving mesh methods for partial differential equations, including the variational approach Brackbill et al. [1]; finite element methods of Millers [2]; moving mesh PDEs of Cao et al. [3], and Ceniceros and Hou [4]; and moving mesh methods based on harmonic mapping of Dvinsky [5] and Li et al. [6, 7]. The main objective of this talk is to develop multi-dimensional AMR methods for the nonlinear Hamilton-Jacobi (H-J) equations:

$$\phi_t + H(x, t, \phi_{x_1}, \dots, \phi_{x_d}) = 0, \quad (1)$$

where  $x \in R^d, t > 0$ . The H-J equations are of practical importance with applications ranging from mathematical finance and differential games to front propagation and image enhancement. For this reason, there have seen many theoretical and numerical studies for the H-J equations in the past two decades. Solutions of H-J equations are continuous and, in the generic case, form discontinuous derivatives in a finite time even with smooth initial conditions. This also introduces great difficulties in obtaining numerical solutions of the H-J equations. In solving the H-J equations (1) with an AMR method, the first difficulty is to find out an appropriate monitor (or control) function. Interpolation is another issue requiring careful attention. The interpolation step and the PDE time-evolution should be well connected so that the higher-order (formal) rate of convergence can be preserved. One of the important applications of our AMR algorithm is the simulation for the geometrical motion [8]. Once the AMR algorithm for the H-J equations is developed, a series of simulations for the geometrical motions may be carried out. To demonstrate the desired effects of the AMR methods, we present in Fig. 1 a numerical simulation for the motion of a simple closed curve, namely boundary of domain “**H**”, by solving a level set equation collapsing with speed proportional to the local curvature. This problem serves as a challenging test problem to numerically verify Grayson’s theorem which claimed that all simple closed curves eventually collapse to a round point [9].

## References

- [1] J.U. Brackbill and J.S. Saltzman, Adaptive zoning for singular problems in two dimensions, *J. Comput. Phys.* 46 (1982), pp. 342–368.
- [2] K. Miller and R.N. Miller, Moving finite element. I, *SIAM J. Numer. Anal.* 18(1981), pp. 1019–1032.
- [3] W.M. Cao, W.Z. Huang and R.D. Russell, An  $r$ -adaptive finite element method based upon moving mesh PDEs, *J. Comput. Phys.* 149 (1999), pp. 221–244.
- [4] H. D. Ceniceros and T. Y. Hou, An efficient dynamically adaptive mesh for potentially singular solutions. *J. Comput. Phys.*, **172**, 609-639 (2001).
- [5] A.S. Dvinsky, Adaptive grid generation from harmonic maps on Riemannian manifolds, *J. Comput. Phys.* 95 (1991), pp. 450–476.
- [6] R. Li, T. Tang, and P.-W. Zhang, Moving mesh methods in multiple dimensions based on harmonic maps. *J. Comput. Phys.* 170 (2001), pp. 562-588.
- [7] R. Li, T. Tang, and P.-W. Zhang, A moving mesh finite element algorithm for singular problems in two and three space dimensions, To appear in JCP.
- [8] S. Osher and J. Sethian, Fronts propagating with curvature dependent speed: Algorithms based on Hamilton–Jacobi formulations, *J. Comput. Phys.*, 79(1988), pp.12–49.

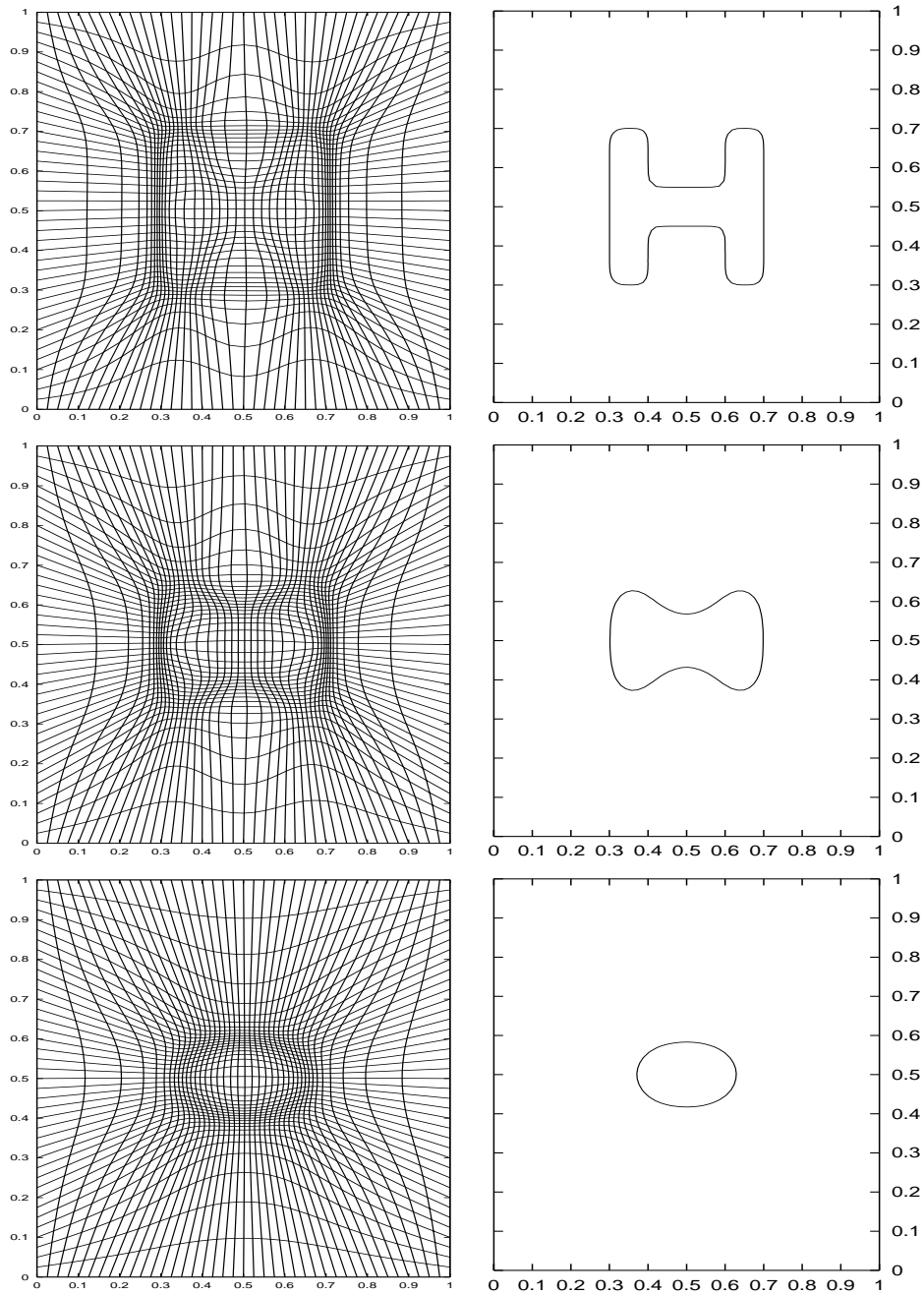


Figure 1: Adaptive mesh and numerical solution for the Grayson's problem:  $t = 0$  (top),  $t = 0.003$  (middle) and  $t = 0.01$  (bottom).

- [9] M. Grayson, The heat equation shrinks embedded plane curves to round points, *J. Diff. Geom.*, 26(1987), pp.285–314.

### **Adaptive Mesh Redistribution Method for Convection-Dominated Problems**

Zhengru Zhang

*Department of Mathematics, Hong Kong Baptist University*

An adaptive mesh method was recently developed by Tang and Tang for solving multi-dimensional hyperbolic conservation laws. In this work, their method will be extended to construct an efficient moving mesh algorithm for nonlinear convection-dominated problems. Our approach includes two independent parts: PDE evolution and mesh re-distribution. In the first part, we transform the underlying equation to the computational domain with fixed regular mesh, then apply second order MUSCL type finite volume methods to approximate the flux and standard central differencing for the diffusion term. The second part is based on a variational principle and the mesh updating is based on an iteration procedure. Particular attention is paid to handling the diffusion terms.

Several numerical examples are provided to demonstrate the efficiency of the proposed algorithm. The numerical experiments for one- and two-dimensional problems suggest that our algorithm is efficient and robust for solving convection-diffusion equations with very small viscosity. For the same resolution, the adaptive mesh redistribution method requires much less grid points than the conventional fixed mesh approach.

### **H-Adaptive Multiscale Schemes for the Compressible Navier-Stokes Equations**

Siegfried Müller\*

*Institut für Geometrie und Praktische Mathematik, RWTH Aachen, Germany*

Philipp Lamby

*Institut für Geometrie und Praktische Mathematik, RWTH Aachen, Germany*

Frank Bramkamp

*Lehr- und Forschungsgebiet für Mechanik, RWTH Aachen, Germany*

We present the main conceptual ingredients and the current state of development of the new solver QUADFLOW for large scale simulations of compressible fluid flow and fluid–structure interaction. In order to keep the size of the discrete problems at every stage as small as possible for any given target accuracy, we employ a multiresolution adaptation strategy that will be described in the first part. In the second part we outline a new mesh generation concept that is to support the adaptive concepts as well as possible. A key idea is to understand meshes as parametric mappings determined by possibly few control points as opposed to store each mesh cell separately. Finally, we present a finite volume discretization which again is to support the adaptation concepts. We conclude with numerical examples of realistic applications demonstrating different features of the solver. The conceptual details are outlined in [1].

## References

- [1] F. Bramkamp, B. Gottschlich–Müller, M. Hesse, Ph. Lamby, S. Müller, J. Ballmann, K.-H. Brakhage, W. Dahmen: *H*-adaptive Multiscale Schemes for the Compressible Navier–Stokes Equations — Polyhedral Discretization, Data Compression and Mesh Generation, Bericht Nr. 207, RWTH Aachen, 2001

### **H-box methods for the approximation of conservation laws on irregular grids and in complex geometries**

Christiane Helzel\*

*Courant Institute, New York, USA*

Marsha J. Berger

*Courant Institute, New York, USA*

We consider the approximation of multidimensional systems of conservation laws on Cartesian grids with embedded irregular boundaries. In order to obtain a stable approximation with explicit finite volume methods using time steps that are appropriate for the regular grid cells, a special treatment of the irregular boundary cells, that may be orders of magnitude smaller than the regular grid cells, is necessary.

Our approach is based on the so-called *h*-box method developed by Berger and LeVeque in [2], [3]. In this scheme a stable approximation of small boundary cells is achieved by constructing fluxes in a way that the flux differences calculated for a boundary cell are of the size of the small irregular cell. They suggested a rotated grid method which has this cancellation property of numerical fluxes. We present a new method in which the cancellation property is obtained by a simpler approach that does not need a rotated grid. In our method all *h*-boxes are constructed in coordinate directions. This is possible by splitting up the boundary flux into components in all coordinate directions.

Although our main interest lies in the construction of multidimensional schemes that can handle embedded boundaries, the study of *h*-box methods in one space dimension provides insight. By looking at the approximation of 1D systems of conservation laws on an irregular grid, we consider the construction of methods that are stable for time steps adequate to a constant reference grid cell length *h*. The numerical grid can contain mesh cells that are orders of magnitude smaller than *h*. We present a high resolution *h*-box method that is based on LeVeque's wave propagation scheme. For the advection equation we can show that this scheme leads to second order accurate approximations of smooth solutions on arbitrary irregular grids. Numerical results confirm the same order of accuracy for the approximation of the Euler equations. The crucial step, in order to construct such accurate high-resolution schemes, lies in the definition of the *h*-boxes that are used in order to approximate the fluxes at small grid cell interfaces. Those values have to be defined by averaging over piecewise linear values of the conserved quantities. An extension of the method for the two-dimensional case will also be described. This irregular grid method is described in [1].

## References

- [1] BERGER M.J., HELZEL, C., LEVEQUE, R.J., *H*-box methods for the approximation of hyperbolic conservation laws on irregular grids, in preparation 2002.
- [2] BERGER M.J., LEVEQUE, R.J., Stable boundary conditions for Cartesian grid calculations, *Computing Systems in Engineering*, 1:305-311, 1990.
- [3] BERGER M.J., LEVEQUE, R.J., A rotated difference scheme for Cartesian grids in complex geometries, *AIAA Paper*, CP-91-1602, 1991.

## 4.7 Monday, Session 4 (morning): Rays and fronts

### Fast sweeping method for Eikonal equations

Hongkai Zhao

*University of California, Irvine, USA*

A simple iterative method, called fast sweeping method, method, for computing the solution of the Eikonal equation  $|\nabla u(x)| = c(x)$  on a Cartesian grid is proposed. The method combines upwind difference and Gauss Seidel iterations with different sweeping order to automatically follow the characteristics of Eikonal equations in certain directions simultaneously. The convergence and error estimates of the fast sweeping method will be analyzed in detail. In particular, it is shown that the number of sweepings for the fast sweeping method depends on  $c(x)$  and the space dimension and is independent of the grid size to achieve certain accuracy. High order schemes, extensions to a class of Hamilton-Jacobi equations and applications will also be discussed.

### An Eulerian Framework for Geometrical Optics Using the Level Set Method

Li-Tien Cheng

*University of California, San Diego, USA*

The level set method has been successfully applied to numerous problems in mathematics and in science dealing with interface motions. This is due mainly to its flexibility and its ability to automatically handle topological changes and resolution. Recently, the level set method has been extended to further handle objects of higher codimension such as curves in three dimensions. We present here the application of this technique to constructing wavefronts in geometrical optics. The wavefronts when viewed in phase space generate Lagrangian submanifolds of high codimension. The Liouville PDE on these objects then gives the desired wavefronts. Operating with a level set representation in phase space provides the underlying Eulerian framework where multivalued wavefronts are handled with ease. We present results for both isotropic and anisotropic wave propagations.

## 4.8 Monday, Session 4 (afternoon): Fronts and the level-set method

### Error Analysis of Difference Methods for Moving Boundary Problems of Hyperbolic Systems

Wen-An Yong

*University of Heidelberg, Germany*

This work is concerned with finite difference methods for moving boundary problems of one-dimensional nonlinear hyperbolic systems. Such problems stem mainly from front tracking methods in computing discontinuity solutions of hyperbolic conservation laws. For our analysis we present a stability theory of difference schemes for initial boundary value problems of algebraic hyperbolic systems. The error estimate follows from a combination of the new stability theory and the asymptotic expansion technique due to Strang.

#### A local level-set concept for front tracking on arbitrary grids

F. Völker\*, R. Vilsmeier and D. Hänel

*Institute of Combustion and Gasdynamics, Germany*

This paper proposes a general multi-dimensional front tracking concept for arbitrary physical problems. The concept is integrated as a module in a basic Finite-Volume solution method (MOUSE: <http://www.vug.uni-duisburg.de/MOUSE/>) for systems of conservation laws on arbitrary grids.

The common basis of the tracking concept is a local level-set method combined with a flux-separation approach at the front. The definition range is dynamic according to the moving front position and restricted to the first two neighbor nodes levels on both sides of the front. The front geometry is described by the value  $G = 0$  of a scalar function  $G(x, y, [z])$  and moved according to an Eulerian transport equation:

$$\frac{\partial G}{\partial t} + \vec{c} \cdot \nabla G = 0 \quad (1)$$

The transport of the front in addition with a two step normalization procedure forms the front tracking algorithm for one time step. For reasons of accuracy the level-set function is normalized to approximately satisfy the slope condition

$|\nabla G| = 1$ , corresponding to a distance function to the front. The normalization procedure involves iterations by pointwise least square approaches and proceeds in two steps: In the first step, the direction of the gradient  $\nabla G^n$  is computed. For a node  $i$  with a restricted number of neighbors  $\tilde{j} \in E_{par}(i)$  the error approach reads:

$$\Phi_{par} = \sum_{\tilde{j} \in E_{par}(i)} \left( \frac{\nabla G_i \cdot \vec{m}_{i\tilde{j}} - (G_{\tilde{j}} - G_i)}{|\vec{m}_{i\tilde{j}}|^{q/2}} \right)^2 \rightarrow \text{minimum} \quad (2)$$

with  $\vec{m}_{i\tilde{j}} = \vec{X}_{\tilde{j}} - \vec{X}_i$  and a distance weighting exponent  $q \geq 0$ .

In the second step

$$\Phi_{hyp} = \sum_{j \in E_{hyp}(i)} \left( \frac{\frac{\nabla G_i^n}{|\nabla G_i^n|} \cdot \vec{m}_{ij} - (G_j - G_i^{n+1})}{|\vec{m}_{ij}|^{q/2}} \right)^2 \rightarrow \text{minimum} \quad (3)$$

the functional value of  $G^{n+1}$  is set to satisfy the slope condition. The result of the second step is a new functional value for  $G$ . Due to dependencies with neighboring nodes, the method is used iteratively. Unfortunately, it is not possible to satisfy the slope condition without slightly altering the actual front position in a linear representation on the edges of the mesh. Additional

corrections are thus performed to preserve the exact front position after normalization. Doing so, the exact slope condition is again voided, which is however more tolerable than a falsified front position itself.

The motion of the front is carried out by an explicit time discretization of equation 1. Assuming a constant slope, the propagation step reads:

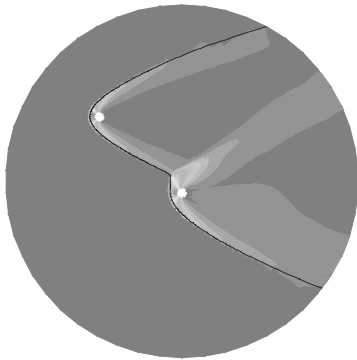
$$G^{n+1} = G^n - \vec{c} \cdot \nabla G^n \Delta t \quad (4)$$

This equation is solved under the assumption of frozen velocity  $\vec{c}$  during a time step. Due to the inaccuracies of the constant slope condition, an additional translation error is introduced. Therefore, above equation is extended by a Taylor expansion for the gradient in normal direction:

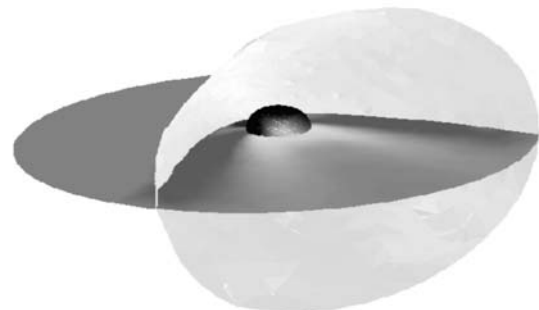
$$G^{n+1} = G^n - \vec{c} \cdot \nabla G^n \Delta t + \frac{1}{2} \Delta t^2 \vec{c} \cdot \frac{\partial \nabla G}{\partial x_n} \quad (5)$$

where  $x_n$  is a locally transformed, normal coordinate direction to the front. According to this modification, the slope condition  $|\nabla G| = 1$  of the level set function is less important, thus lowering the need for large iteration numbers within the normalization procedure and assuring a good accuracy of the propagation.

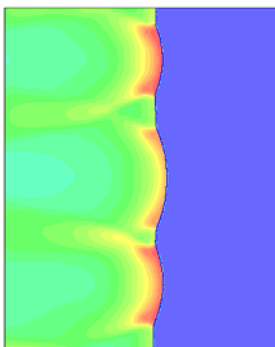
Above methods will be demonstrated by a variety of gas-dynamical stationary and transient shock wave computations in 2D and 3D.



Flow past a 2D pair of cylinders, inviscid,  $Ma_\infty = 3$ , tracked bow shock.



Flow past a 3D sphere, inviscid,  $Ma_\infty = 2$ , tracked bow shock.



Example for a transient detonation wave with tracked front shock wave.

### Eulerian Ray Tracing and Applications to Grid Generation

Patrizia Bagnerini

*Laboratoire de Mathématiques CNRS n.6621, Université de Nice, France*

We consider the Hamilton-Jacobi equation on a domain  $\Omega \subset R^2$ , and the bicharacteristics, i.e. the integral curves of the associated Hamiltonian system:

$$\dot{x}(t) = H_p(x, p), \dot{p}(t) = -H_x(x, p). \tag{1}$$

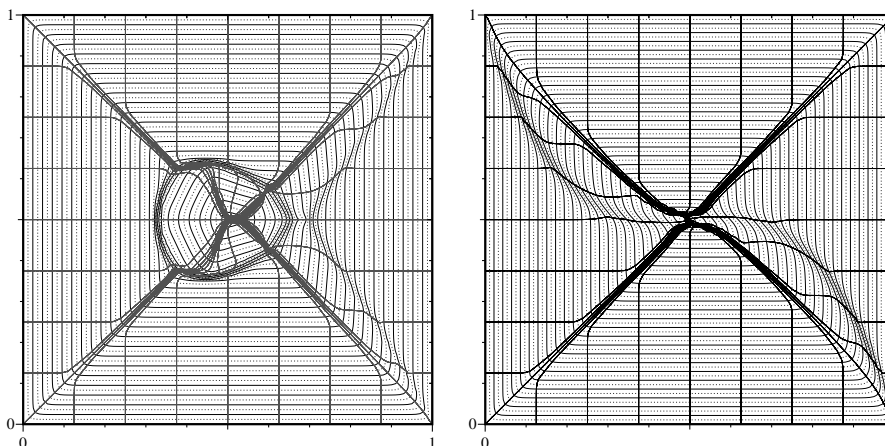
In order to generate meshes, but also for the other applications (rays in geometrical optics, etc ..), it would be useful to compute the rays in an Eulerian way. So, following an idea of J.-D. Benamou [3], we label each ray by a parameter  $\theta$  and thus we compute a function  $\theta = \theta(s, t)$ ,  $\theta : \Omega \rightarrow R$ , whose level sets are the rays.  $\theta$  is then solution to the problem:

$$\begin{cases} F = \frac{\partial H}{\partial p} \cdot \nabla \theta = 0 & \text{in } \Omega \\ \theta(x) \text{ given } \in [0, 2\pi[ & \text{on } \partial\Omega. \end{cases} \tag{2}$$

In principle, this approach allows to obtain directly all the bicharacteristic curves as the level sets of a function  $\theta$ , instead of solving a system of ODE for every source point belongs to  $\partial\Omega$ . One of motivations is the generation of adaptive meshes, and then we apply the method to the Eikonal Riemannian equation (see [1, 2]), with a suitable Riemannian metric which allows to refine the mesh in regions typically where the the function we want to approximate is stiff.

Recently, fast algorithms for computing the viscosity solution of different classes of Hamilton-Jacobi equations have been developed, see in particular [4, 5, 6]. Our goal in this work is to compute, if possible, at the same time, the viscosity solution of the anisotropic Hamilton-Jacobi equation and the bicharacteristics, corresponding to the level sets of the function  $\theta$ . As noted in [4, 5, 6], it is very delicate to use the bicharacteristics (the optimal trajectories of the corresponding min-time control problem) to construct an efficient method for computing the viscosity solution  $u$ : the characteristic and the gradient direction of  $u$  are different and a causality property does not exist: it is no longer possible to decouple the system by computing the mesh points in the ascending order.

The same type of problem arises in the computing of the equation (2) and so we use a weaker approximate causality property [4] and a Fast Marching type of algorithm for computing the function  $\theta$  on  $\Omega$ . In the following figures, we show, for an anisotropic problem, the levels curves of the viscosity solution  $u$  and of the solution  $\theta$  of (2), which allow to construct the basic structure of an adaptive mesh.



### References

- [1] Hoch Ph., Rascle M., *Hamilton-Jacobi Equation on a Manifold and Applications to Grid Generation or Refinement*, to appear SIAM J. Sc. Computing

- [2] Bagnerini P., Hoch Ph., Rascle M., *The Eikonal Equation on a Manifold. Applications to Grid Generation or Refinement*, Proceedings of the Eight Conference on Hyperbolic Problems, Magdeburg, Feb-March 2000
- [3] Benamou J.-D. , *Big ray tracing: Multivalued travel time field computation using viscosity solution of eikonal equation*, J. Comp. Physics, 128:463-474, 1996
- [4] Sethian J.A., Vladimirsky A., *Ordered Upwind Methods for Static Hamilton-Jacobi Equations: Theory and Algorithms*, PAM-792 Report, June 2001
- [5] Tsai Y.R., Cheng L., Osher S., Zhao H., *Fast Sweeping Algorithm of a Class of Hamilton-Jacobi Equations*, 01-27 UCLA Report, October 2001
- [6] Osher, S., Fedkiw, R. P. , *Level set methods: an overview and some recent results*, J. Comput. Physics, 169 no. 2:463–502

### **A Level Set Method for Computing Discontinuous Solutions of a Class of Hamilton-Jacobi Equations**

Yen-Hsi Richard Tsai\* and Stanley Osher

*Department of Mathematics, University of California Los Angeles, Los Angeles, California 90095*

Yoshikazu Giga

*Department of Mathematics, University of Hokkaido, Japan*

We introduce finite difference methods to compute the L-solution and the proper viscosity solution recently proposed by Y. Giga for semi-discontinuous solutions to a class of Hamilton-Jacobi equations. By embedding the graph of the solution as the zero level curve of a continuous function in one dimension higher, we can treat the corresponding level set equation using the viscosity theory introduced by Crandall and Lions. However, we need to pay special attention both analytically and numerically to prevent the zero level curve from overturning so that it can be interpreted as the graph of a function. We couple our numerical methods with a singular diffusive term which is essential to computing solutions to a general class of HJ equations that includes scalar conservation laws. With this singular viscosity, our numerical methods do not require the divergence structure of equations and do apply to more general equations developing shocks other than conservation laws.

## 4.9 Monday, Session 5 (morning): Numerical methods for MHD I

### Multi-Dimensional Upwinding Method for the MHD-equations

Michael Fey\* and Manuel Torrilhon

*Seminar for Applied Mathematics, ETH Zürich, Switzerland*

#### Introduction

Many flows, particularly astrophysical flows, are electrically conducting, and the electromagnetic forces can be of the same order as the hydrodynamic forces. The governing equations of **magneto**hydrodynamics (MHD) basically merges the Euler equations of gas dynamics with the Maxwell equations of electromagnetics. A feature of the MHD-equation, in contrast to the Euler system, is the additional constrain  $\text{div}(\mathbf{B}) = 0$  on the magnetic field. This constrain does not introduce an elliptic character into the equation but is intrinsically represented as  $\partial_t(\text{div}(\mathbf{B})) = 0$ . Thus the system of equations automatically meets the constrain  $\text{div}(\mathbf{B}) = \text{const}$ . If this constant is zero it remains zero for all times.

Based on the ideas of multidimensional upwinding, we will present an explicit multi-dimensional upwind scheme for the MHD-equations, which conserves  $\text{div}(\mathbf{B})$  according to a numerical divergence-operator and whos timestep is fully local. Properties of the equations are discussed to show the influence of different choices of wave models.

#### Multi-Dimensional Upwinding

We will briefly summarize the idea of multi-dimensional upwinding. The idea is an extension of the **Method of Transport** (MoT) for non-linear systems of conservation laws. The method consists of two independent parts: The decomposition of the non-linear system of conservation laws into a set of linear systems and the proper solution of these linear systems.

A general system of conservation laws can be written as

$$\mathbf{U}_t + \nabla \cdot \underline{\mathbf{F}}(\mathbf{U}) = 0 \quad (1)$$

with the vector  $\mathbf{U}$  of the conserved quantities and the flux matrix  $\underline{\mathbf{F}}$ . Decomposition means, that we look for  $k$  vectors  $\mathbf{S}_i = \mathbf{S}_i(\mathbf{U})$  and velocities  $\mathbf{a}_i = \mathbf{a}_i(\mathbf{U})$  that the two conditions

$$\mathbf{U} = \sum_{i=1}^k \mathbf{S}_i \quad \text{and} \quad \underline{\mathbf{F}}(\mathbf{U}) = \sum_{i=1}^k \mathbf{S}_i \mathbf{a}_i^T \quad (2)$$

holds. The actual linearisation consists in the decoupling of the functions  $\mathbf{S}_i$  and  $\mathbf{a}_i$  from  $\mathbf{U}$ . The system (1) can approximately solved by the set of linear equations

$$\begin{aligned} (\mathbf{S}_i(\mathbf{x}, \tau))_\tau + \nabla \cdot (\mathbf{S}_i(\mathbf{x}, \tau) \mathbf{a}_i^T(\mathbf{x})) &= 0 \quad i = 1, \dots, k \\ \mathbf{S}_i(\mathbf{x}, 0) &= \mathbf{S}_i(\mathbf{U}(\mathbf{x}, t)) \quad \mathbf{a}_i(\mathbf{x}) = \mathbf{a}_i(\mathbf{U}(\mathbf{x}, t)). \end{aligned} \quad (3)$$

The solution after time  $\Delta t$  is

$$\mathbf{U}(\mathbf{x}, t + \Delta t) = \sum_{i=1}^k \mathbf{S}_i(\mathbf{x}, \Delta t).$$

We call (3) the advection form of (1). As a numerical scheme for the non-linear system we basically need a scheme for the scalar linear system.

Note, that with simple extensions or rewriting of the equations most of the existing schemes can be written in this framework. For example, writing the equations in terms of the residual  $res = -\nabla \cdot \underline{\mathbf{F}}(\mathbf{U})$ , we get a conservation law of the form

$$res_t + \nabla \cdot \left( \frac{d\underline{\mathbf{F}}}{d\mathbf{U}} \cdot res \right) = 0.$$

Applying the framework to this representation will include the flux difference and residual splitting methods.

### The MHD-Equations

The MHD-equations can be written as conservation laws (1) with

$$\mathbf{U} = \begin{pmatrix} \rho \\ \rho \mathbf{u} \\ \mathbf{B} \\ E \end{pmatrix} \quad \text{and} \quad \mathbf{F} = \begin{pmatrix} \rho \mathbf{u}^T \\ \rho \mathbf{u} \mathbf{u}^T + \left( p + \frac{|\mathbf{B}|^2}{2} \right) \mathbf{I} - \mathbf{B} \mathbf{B}^T \\ \mathbf{B} \mathbf{u}^T - \mathbf{u} \mathbf{B}^T \\ \left( E + p + \frac{|\mathbf{B}|^2}{2} \right) \mathbf{u}^T - (\mathbf{u} \cdot \mathbf{B}) \mathbf{B}^T \end{pmatrix} \quad (4)$$

where  $\rho$  denotes the density,  $\mathbf{u}$  the velocity vector,  $\mathbf{B}$  the magnetic field and  $E$  the total energy. The pressure  $p$  is related to the conserved quantities by the equation of state

$$E = \frac{p}{\gamma - 1} + \rho \frac{|\mathbf{u}|^2}{2} + \frac{|\mathbf{B}|^2}{2} \quad (5)$$

Even though a decompositions of the MHD-equations into advection form (3) can be found, it is not possible to construct a divergence-free scheme with this ansatz. The advection form (3), like any other planar wave decomposition is unable to control the divergence in the linear equations except for the simple one-dimensional case where the constrain reduces to  $B_1 = \text{const}$ . Thus, the constrain can only be fulfilled as a combination of different waves. We will discuss the implications and disadvantages of this approach.

To take care of the special form of the equation we add a new advection type wave to the decomposition that is able to control the divergence. We use  $l$  vectors  $\mathbf{T}_j = \mathbf{T}_j(\mathbf{U})$  and velocities  $\mathbf{b}_j = \mathbf{b}_j(\mathbf{U})$  such that

$$\mathbf{B} = \sum_{j=1}^l \mathbf{T}_j \quad \text{and} \quad \mathbf{B} \mathbf{u}^T - \mathbf{u} \mathbf{B}^T = \sum_{j=1}^l (\mathbf{T}_j \mathbf{b}_j^T - \mathbf{b}_j \mathbf{T}_j^T).$$

Again we decouple  $\mathbf{T}_j$  from  $\mathbf{B}$  and  $\mathbf{b}_j$  from  $\mathbf{U}$  and can approximately solve the equations for the magnetic field in (4) by the set of equations

$$\begin{aligned} (\mathbf{T}_j(\mathbf{x}, \tau))_\tau + \nabla \cdot (\mathbf{T}_j(\mathbf{x}, \tau) \mathbf{b}_j^T(\mathbf{x}) - \mathbf{b}_j(\mathbf{x}) \mathbf{T}_j^T(\mathbf{x}, \tau)) &= 0 \quad j = 1, \dots, l \\ \mathbf{T}_j(\mathbf{x}, 0) &= \mathbf{T}_j(\mathbf{B}(\mathbf{x}, t)) \quad \mathbf{b}_j(\mathbf{x}) = \mathbf{b}_j(\mathbf{U}(\mathbf{x}, t)) \end{aligned} \quad (6)$$

and the solution after time  $\Delta t$  is

$$\mathbf{B}(\mathbf{x}, t + \Delta t) = \sum_{j=1}^l \mathbf{T}_j(\mathbf{x}, \Delta t).$$

This linear equations share the same constrain as the nonlinear system. We will discuss the properties of the linear system and show the basic ideas to derive a multi-dimensional divergence-free upwind method.

### Decomposition of the MHD-equations

The last part of the method is to find a proper decomposition of the MHD equations into the two types of advection equations. Since the linear equations (6) introduce no divergence into the solution nor will the sum of several of them. Thus, we can freely combine these waves to model the physics of the problem.

On the basis of properly scaled eigenvectors we will show possible decompositions. Special emphasis is set on the multidimensional character and a smooth transition in critical points.

Some numerical results for the most simple decomposition will be shown.

## Efficient Higher–Order Finite Volume Schemes for (Real Gas) Magnetohydrodynamics

Matthias Wesenberg\* and Andreas Dedner

*Institut für Angewandte Mathematik, Universität Freiburg, Freiburg, Germany*

### Introduction

The equations of magnetohydrodynamics (MHD) are a model for a compressible, inviscous, and electrically conducting gas in the presence of a magnetic field. They are derived from the Euler equations of gas dynamics and the Maxwell equations and can be written in divergence form:

$$\partial_t \rho + \nabla \cdot (\rho \mathbf{u}) = 0 \quad (\text{conservation of mass}), \quad (1a)$$

$$\partial_t (\rho \mathbf{u}) + \nabla \cdot (\rho \mathbf{u} \mathbf{u}^T + \mathcal{P}) = 0 \quad (\text{conservation of momentum}), \quad (1b)$$

$$\partial_t \mathbf{B} + \nabla \cdot (\mathbf{u} \mathbf{B}^T - \mathbf{B} \mathbf{u}^T) = 0 \quad (\text{induction equations}), \quad (1c)$$

$$\partial_t (\rho e) + \nabla \cdot (\rho e \mathbf{u} + \mathcal{P} \mathbf{u}) = 0 \quad (\text{conservation of energy}), \quad (1d)$$

$$\nabla \cdot \mathbf{B} = 0 \quad (\text{divergence constraint}). \quad (1e)$$

For the density  $\rho$ , the velocity  $\mathbf{u} = (u_x, u_y, u_z)^T$ , and the magnetic field  $\mathbf{B} = (B_x, B_y, B_z)^T$  the total energy  $e$  is the sum of the internal, kinetic, and magnetic energies:

$$e = \varepsilon + \frac{1}{2} |\mathbf{u}|^2 + \frac{1}{8\pi\rho} |\mathbf{B}|^2. \quad (2)$$

If  $\mathcal{I}$  denotes the unit tensor, the pressure tensor  $\mathcal{P}$  is defined as

$$\mathcal{P} := \left( p + \frac{1}{8\pi} |\mathbf{B}|^2 \right) \mathcal{I} - \frac{1}{4\pi} \mathbf{B} \mathbf{B}^T. \quad (3)$$

The gas pressure  $p(\tau, \varepsilon)$  is given by a suitable *equation of state* (EOS), where  $\tau := 1/\rho$  is the specific volume. The simplest example is the EOS of a perfect gas

$$p(\tau, \varepsilon) = (\gamma - 1) \frac{\varepsilon}{\tau}, \quad (4)$$

which for  $\gamma = 1.4$  is a model for air if the pressure and the temperature are moderate. For low temperatures and high pressures the EOS also has to respect the influence of intermolecular forces. One possible model in this situation is the van der Waals–EOS

$$p(\tau, \varepsilon) = \frac{R (\varepsilon - \varepsilon_0 + \frac{a}{\tau})}{c_V (\tau - b)} - \frac{a}{\tau^2} \quad (5)$$

for suitably chosen constants  $a, b, R, c_V$ , and  $\varepsilon_0$ .

The system (1) is hyperbolic and has to be closed by suitable initial and boundary conditions. To ensure the divergence constraint (1e) in multidimensional simulations we use the technique presented in [DKK<sup>+</sup>02].

In [DW01] we introduced two classes of approximate one–dimensional Riemann solvers for the real gas MHD equations (1), which we use as interface fluxes in our multidimensional codes. Motivated by the work in [BGH00] for the Euler equations of gas dynamics (that is, (1a), (1b), (1d), and (3) with  $\mathbf{B} \equiv 0$ ), the first approach takes advantage of the fact that the structure of the MHD eigensystem in primitive variables is completely *independent* of the EOS chosen. Only the gas pressure  $p$  and the speed of sound  $c_s$  are EOS–dependent functions. Thus in principle we can use the same Riemann solvers as for the perfect gas law (4). However, since conversions between primitive and conservative variables can be quite expensive, it pays off to use primitive variables within the schemes wherever possible. The RGDW–solver which was presented in [DW01] and which is derived from the perfect gas solver originally introduced in [DW95] completely follows these ideas.

The second class of solvers is based on the energy relaxation approach for Euler [CP98], which can also be extended to MHD. For obtaining a numerical flux for the real gas system (1) we choose a suitable value for  $\gamma$ , reuse an arbitrary numerical flux for the perfect gas (4) and perform an relaxation step for the total energy. By means of this approach the extension of a perfect gas code to the real gas case becomes very simple.

In this communication we present recent extensions of our previous work [DW01] and [DKRW01]. Due to the enormous memory requirements of a fixed table for an EOS in practical computations, we suggest the use of *adaptively refined* tables, see Section 4.9. Within a comparison of various MHD solvers for perfect gases, our new MHD–HLLM scheme turned out to be the most efficient one, see Section 4.9. We also discuss potential advantages of performing the linear reconstruction in primitive variables rather than in conservative variables. While in one space dimension it is straightforward to implement a scheme which shows second order convergence in numerical tests, this is a delicate task in two space dimensions. We identified two main obstacles on unstructured (triangular) grids in 2D: inappropriate limiters and a tremendous influence of the grid structure. Both issues are addressed in Section 4.9. We suggest a new limiter which guarantees an oscillation–free reconstruction and which leads to more efficient higher order schemes.

### Tabularized Equations of State

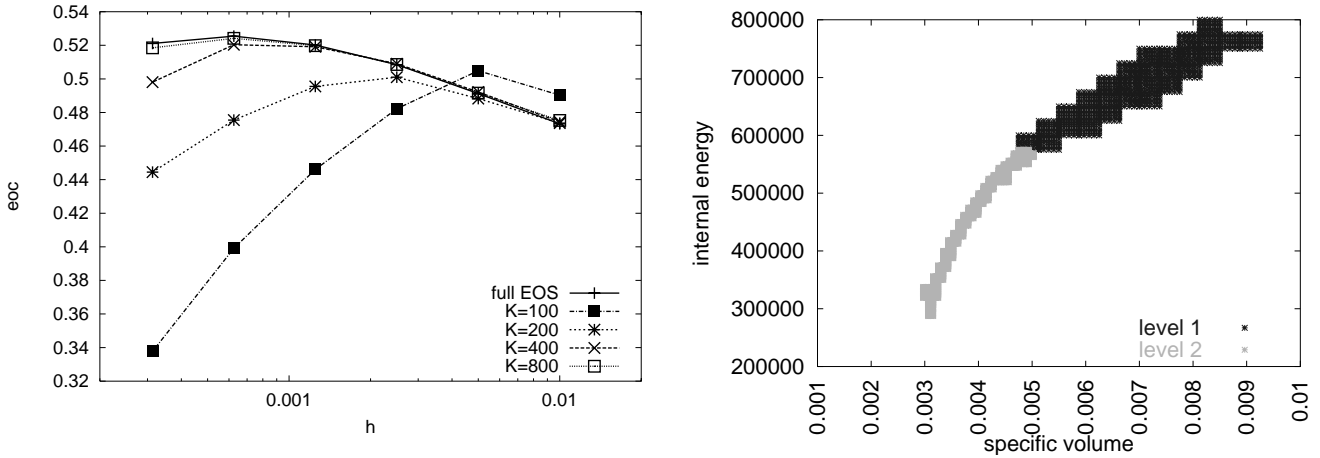


Figure 1: Left: Results of the first order RGDW scheme for a van der Waals shock tube problem; grid spacing  $h$  versus experimental order of convergence (eoc) for full EOS (solid line) and tables with resolution  $K \times K$  (dotted/dashed lines). Right: Levels of refinement in an adaptive table for  $p$  as function of  $\tau$  and  $\varepsilon$  for the same problem.

In many applications the evaluation of the EOS is possible for arbitrary values of  $\tau$  and  $\varepsilon$ , but expensive due to the iterative procedures required for computing  $p(\tau, \varepsilon)$ . In this situation for the sake of computational efficiency one has to refrain from a direct evaluation of the EOS and store selected EOS values in a table instead. However, the table resolution cannot be chosen independent of the grid resolution, see Fig. 1 left. In order to save memory, we use an adaptive table. This pays off since typically EOS values are only required in the vicinity of the table’s “diagonal”, see Fig. 1 right. For the solar physical MHD problem with a partially ionized plasma considered in [Vol02] we found that the use of an EOS table reduces the computational costs by 90%. Moreover, to achieve a deviation from the exact EOS of less than 1.5%, we would need a cartesian table with 25 million entries; with our adaptive strategy we save 70% of memory.

### Efficiency of One–dimensional Schemes

The classical HLL–solver only resolves the two fastest waves of the underlying one–dimensional system of PDEs accurately, while the waves in between are strongly damped. In [EMRS91] the Euler–HLL–scheme was modified (HLLM–scheme) by adding some anti–diffusion terms which improve the resolution of these waves significantly. Our new MHD–HLLM solver is an extension of these ideas to MHD; all but the fast magnetoacoustic waves are affected by anti–diffusion terms. If the magnetic field  $\mathbf{B}$  vanishes, the MHD–HLLM solver coincides with the Euler–HLLM solver. For a perfect gas MHD–HLLM turned out to be the most efficient solver considered in our comparison for both smooth and non–smooth problems. This holds if the MHD–HLLM flux is used either within a first order one–dimensional finite volume scheme or within a second order scheme based on linear reconstruction with minmod limiter and Runge–Kutta time integration. Some results of MHD–HLLM in comparison with the DW–scheme which is based on [DW95] can be found in Fig. 2. In the real gas case the RGDW–solver introduced in [DW01] may be more efficient for some problems since this solver also works well in primitive variables, whereas for the sake of robustness we implemented our real gas MHD–HLLM solver (RG–HLLM) completely

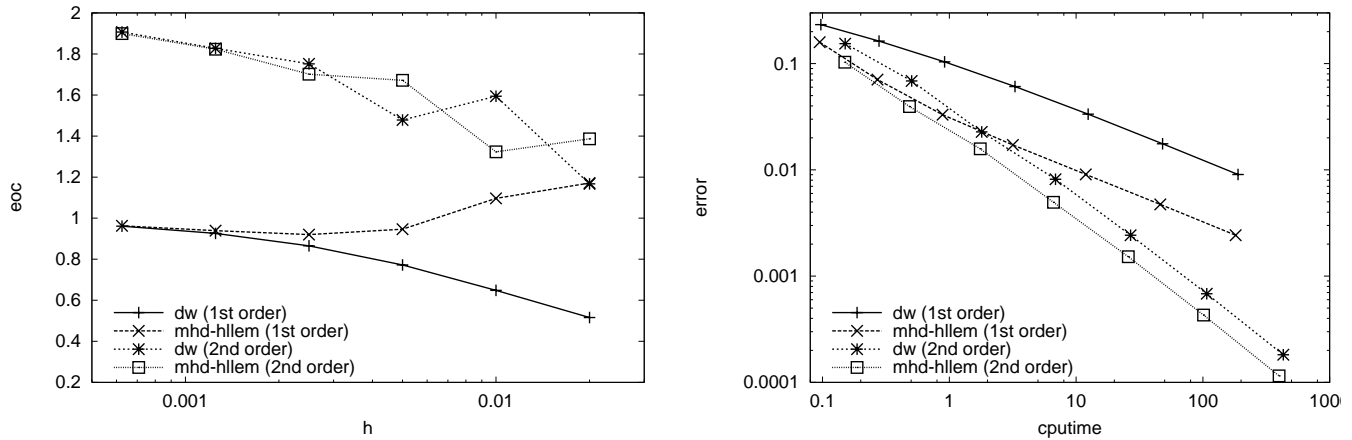


Figure 2: Results of the first and second order DW and MHD–HLEEM scheme in 1d for a smooth advection problem in the perfect gas case. Left: grid spacing  $h$  versus experimental order of convergence (eoc). Right: computational efficiency, that is, cputime versus error.

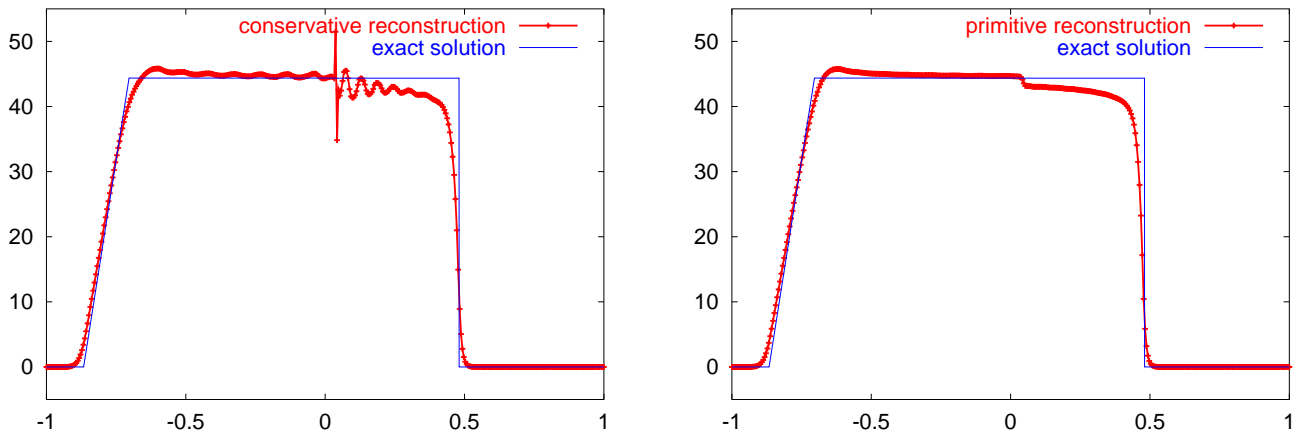


Figure 3: Results of the second order RGDW scheme for a van der Waals shock tube problem; spatial position  $x$  versus  $u_x$ . Across the contact discontinuity  $u_x$  is constant (solid lines). The reconstruction in conservative variables introduces spurious oscillations (left), which do not occur if we reconstruct in primitive variables.

in conservative variables. Thus up to now for RG–HLEEM many (potentially) expensive conversions between primitive and conservative variables are required.

Numerical tests show that a reconstruction of the constant volume data in conservative variables can cause spurious oscillations. In the example considered in Fig. 3 this is due to the fact that across a contact discontinuity the primitive variables velocity and pressure have to be constant, which does not hold for the conservative quantities momentum and total energy. Thus a reconstruction in primitive variables cures this problem, see Fig. 3 right. Note that the finite volume scheme is conservative for both choices of variables.

In two and three spatial dimensions dynamical local grid adaption is commonly regarded as a powerful tool for saving both main memory and computational time. However, in view of the problems discussed in the next section, it is not clear if in general such second order schemes will indeed be more efficient in terms of error versus runtime ratio than schemes on a fixed grid. We try to answer this question by one– and two–dimensional tests.

### Efficiency of Two–dimensional Schemes

The basic idea of extending a first order finite volume scheme to second order consists of two steps. For each element and each scalar quantity one constructs a linear function, which is then used for the evaluation of the one–dimensional fluxes at the interfaces. For the time integration one uses a standard second order accurate Runge–Kutta method. For the reconstruction

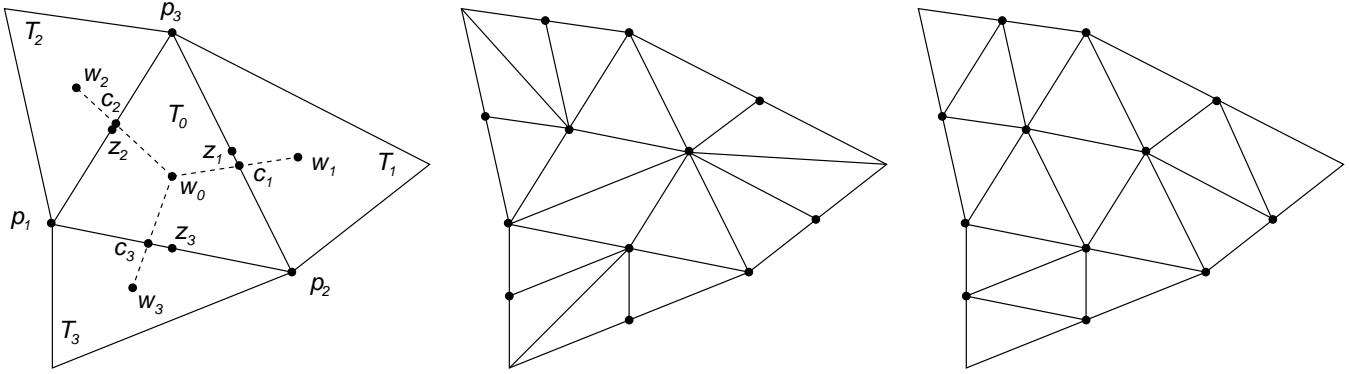


Figure 4: Notation used for the DEO-reconstructions (left); grid after two bisections (middle) and after the quartering of each triangle (right).

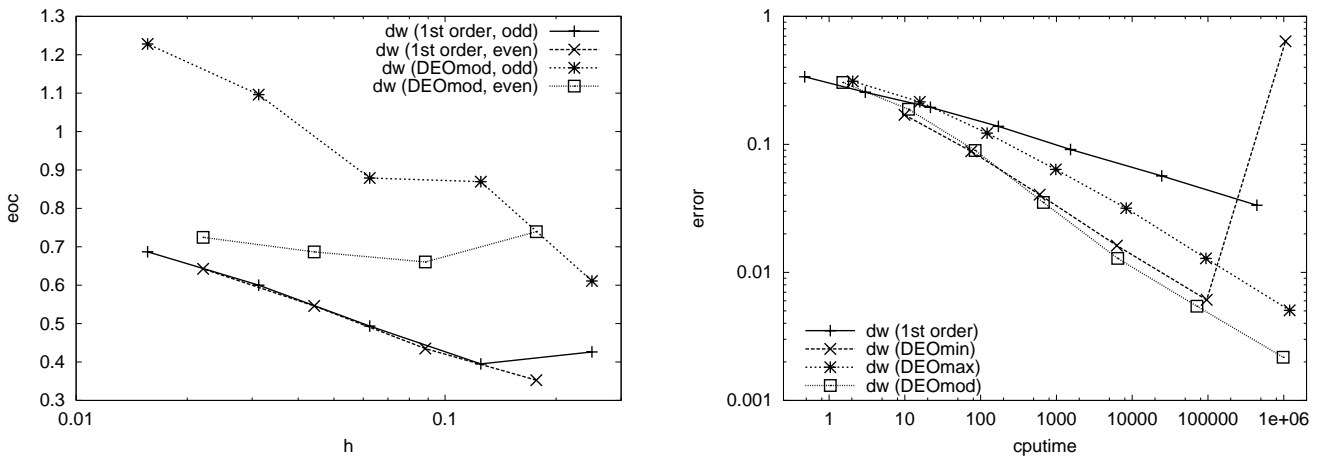


Figure 5: Results of the first and second order DW scheme in 2d for a smooth advection problem in the perfect gas case. Left: The experimental order of convergence is significantly different if the number of bisections is odd or even. Right: The computational efficiency of the schemes with DEO-reconstruction strongly depends on the limiter applied.

in space we follow the approach in [DEO92], since it requires only information from the triangle itself and its three direct neighbours. (A small domain of dependence is important for an efficient parallelization.) We found that both limiters proposed in [DEO92] suffer from serious shortcomings. The choice of the linear function with the gentlest gradient in the DEOmin-approach can be more restrictive than necessary, whereas the missing limitation can introduce oscillations. On the other hand, the DEOmax-limitation still admits oscillations since the values of the *reconstructions* in the neighbours are not taken into account. At the same time, any limited linear reconstruction should recover an initially linear function exactly. Since in general triangular grids the side midpoints  $z_i$  and the intersection points of the barycenter connections with the corresponding side  $c_i$  do not coincide (see Fig. 4 left), this does not hold for the DEOmax-approach.

Our new DEOmod-approach cures all of the previously described problems. We can prove that linear functions are exactly recovered and that DEOmod guarantees oscillation-free reconstructions in the sense

$$|U_0 - L_0(c_i)| + |L_i(c_i) - U_i| \leq |U_0 - U_i| \quad \text{for } 1 \leq i \leq 3$$

if  $U_0, \dots, U_3$  denote the volume values in  $w_0, \dots, w_3$ .

For the smooth advection problem considered in Figs. 5 and 6, the DEOmod-approach is clearly the most efficient one, see Fig. 5 right. If we quarter all triangles within each refinement step as in Fig. 4 right, the experimental order of convergence (eoc) using DEOmod is clearly larger than 1, and as in 1d the second order MHD-HLLEM scheme is the most efficient solver, see Fig. 6. However, if we bisect the triangles with each refinement as in Fig. 4 middle, the results strongly differ depending on whether the number of grid refinements is odd or even, see Fig. 5 left. Since this is only one of the various dependencies on the grid we encountered, the efficiency of locally adaptive second order schemes becomes an urgent question.

## Acknowledgements

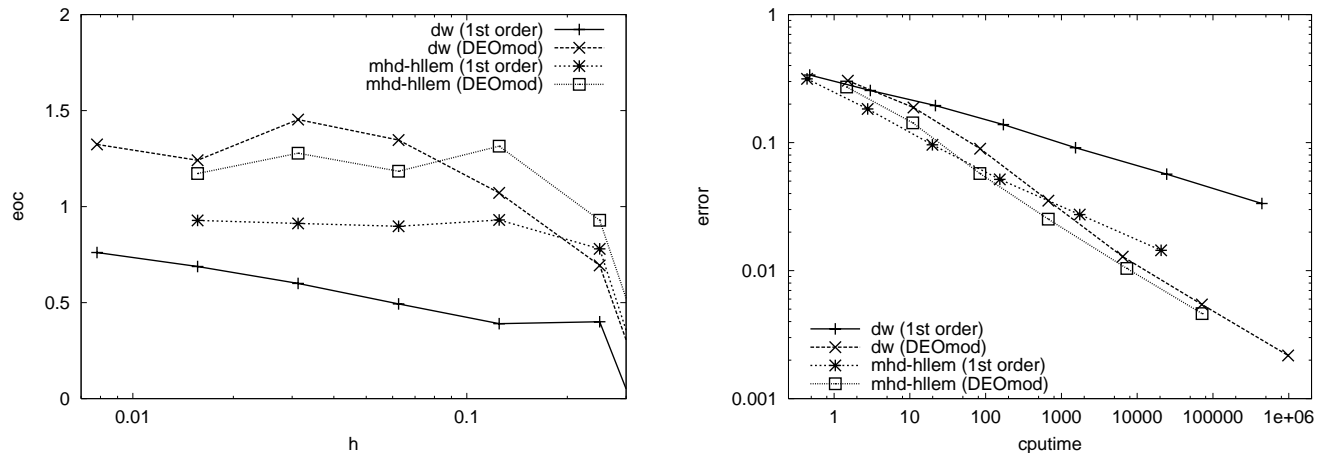


Figure 6: Results of the first and second order DW and MHD–HLLEM scheme in 2d for a smooth advection problem in the perfect gas case. Left: grid spacing  $h$  versus experimental order of convergence (eoc). Right: computational efficiency.

The authors were supported by the DFG priority research program ANumE.

## References

- [BGH00] T. Buffard, T. Gallouet, and J. M. Herard, *A sequel to a rough Godunov scheme: Application to real gases*, *Comput. Fluids* (2000), no. 29, 813–847.
- [CP98] F. Coquel and B. Perthame, *Relaxation of energy and approximate Riemann solvers for general pressure laws in fluid dynamics*, *SIAM J. Numer. Anal.* **35** (1998), no. 6, 2223–2249.
- [DEO92] L.J. Durlofsky, B. Engquist, and S. Osher, *Triangle based adaptive stencils for the solution of hyperbolic conservation laws*, *J. Comput. Phys.* **98** (1992), no. 1, 64–73.
- [DKK<sup>+</sup>02] A. Dedner, F. Kemm, D. Kröner, C.-D. Munz, T. Schnitzer, and M. Wesenberg, *Hyperbolic divergence cleaning for the MHD equations*, *J. Comput. Phys.* **175** (2002), no. 2, 645–673, doi:10.1006/jcph.2001.6961.
- [DKRW01] A. Dedner, D. Kröner, C. Rohde, and M. Wesenberg, *Godunov–type schemes for the MHD equations*, *Godunov Methods: Theory and Applications* (E.F. Toro, ed.), Kluwer Academic/Plenum Publishers, November 2001, pp. 209–216.
- [DW95] W. Dai and P.R. Woodward, *A simple Riemann solver and high–order Godunov schemes for hyperbolic systems of conservation laws*, *J. Comput. Phys.* **121** (1995), no. 1, 51–65.
- [DW01] A. Dedner and M. Wesenberg, *Numerical methods for the real gas MHD equations*, *Hyperbolic Problems: Theory, Numerics, Applications* (Basel) (H. Freistühler and G. Warnecke, eds.), *International Series of Numerical Mathematics*, vol. 140, Birkhäuser, 2001, Eighth International Conference in Magdeburg, February/March 2000, pp. 287–296.
- [EMRS91] B. Einfeldt, C.D. Munz, P.L. Roe, and B. Sjögreen, *On Godunov–type methods near low densities*, *J. Comput. Phys.* **92** (1991), no. 2, 273–295.
- [Vol02] P. Vollmöller, *Untersuchung der Wechselwirkung von Magnetfeldkonzentrationen und konvektiven Strömungen mit dem Strahlungsfeld in der Photosphäre der Sonne*, Dissertation, Max–Planck–Institut für Aeronomie / Universität Göttingen, Göttingen, 2002.

## 4.10 Monday, Session 5 (afternoon): Numerical methods for MHD II

### A Wave Propagation Method with Constrained Transport for the Shallow Water Magnetohydrodynamic Equations

James Rossmannith

*Department of Applied Mathematics, University of Washington, USA*

The ideal magnetohydrodynamic (MHD) equations are important in modeling phenomena in a wide range of applications including space weather, solar physics, laboratory plasmas, and general relativistic fluid flows. Apart from the specific challenges that each one of these applications provides, there are two main difficulties that arise when integrating the MHD equations:

1. The magnetic field should be kept divergence-free from time step to time step in accordance with Maxwell's equations.
2. The numerical update should produce a non-oscillatory solution near discontinuities.

Developing numerical methods that overcome these difficulties is hindered by the fact that the MHD system has a complicated eigenstructure which can become non-strictly hyperbolic in certain regions of the flow. For this reason, it is important to have a model system that retains the divergence-free and non-oscillatory challenges from the MHD equations, but has a simpler eigenstructure and avoids complications in regions of non-strict hyperbolicity.

Gilman [3] introduced a simplified version of the MHD equations called the *shallow water magnetohydrodynamic* (SMHD) equations. This system is analogous to the shallow water equations in the context of hydrodynamics. In order to obtain this system, the fluid is assumed to be a thin layer of constant density that is in magnetohydrostatic balance in the vertical direction. After applying these approximations, the resulting MHD equations are depth averaged to give the lower dimensional SMHD equations:

$$\partial_t \begin{bmatrix} h \\ h\mathbf{u} \\ h\mathbf{B} \end{bmatrix} + \nabla \cdot \begin{bmatrix} h\mathbf{u} \\ h\mathbf{u} \otimes \mathbf{u} - h\mathbf{B} \otimes \mathbf{B} + \frac{1}{2}gh^2\mathcal{I} \\ h\mathbf{u} \otimes \mathbf{B} - h\mathbf{B} \otimes \mathbf{u} \end{bmatrix} = 0 \quad (1)$$

$$\nabla \cdot (h\mathbf{B}) = 0, \quad (2)$$

where  $\nabla = (\partial_x, \partial_y)$ ,  $\otimes$  is the outer product,  $\mathcal{I}$  is the identity matrix, and  $g$  is the gravitational constant. The unknowns in the above equation are the height  $h$ , the magnetic field  $\mathbf{B} = (B_1, B_2)$ , and the velocity field  $\mathbf{u} = (u_1, u_2)$ . The eigenvalues of the flux Jacobian in the  $\ell^{\text{th}}$  direction are given by

$$\lambda_{1,4} = u_\ell \mp \sqrt{B_\ell^2 + gh} \quad (3)$$

$$\lambda_{2,3} = u_\ell \mp B_\ell. \quad (4)$$

The  $\lambda_{1,4}$  fields are known as the *magneto-gravity waves* and are genuinely nonlinear, while the  $\lambda_{2,3}$  fields are known as the *Alfvén waves* and are linearly degenerate. It should be noted here that this system fails to be strictly hyperbolic in the  $\ell^{\text{th}}$  direction if  $B_\ell = 0$ . In this case,  $\lambda_2 = \lambda_3$  and the two Alfvén waves collapse into a single wave, sometimes referred to as the *Rossby wave*. This non-strict hyperbolicity is caused by the merger of two linearly degenerate waves; and therefore, unlike the non-strict hyperbolicity in the MHD equations, it causes no numerical difficulties. Instead, the numerical problems that arise when solving the SMHD system are precisely those stated above: a divergence-free constraint must be maintained during each time step and the update should be non-oscillatory. For these reasons, the focus of this paper is to develop a numerical method for solving the SMHD equations.

The SMHD equations not only require many of the same numerical techniques as the MHD equations, but are important as a mathematical model in their own right. They have been used by Gilman [3] to model the solar tachocline. The solar tachocline is a layer with thickness of about 2%-5% of the solar radius and it separates the convective zone from the radiative zone. It is believed that magnetic fields originating in this thin layer are responsible for solar flares and sunspots; and furthermore, it is believed that mathematical models such as the SMHD equations can be used to gain insight in the dynamics of the tachocline. To gain this insight, accurate and efficient numerical solution techniques must be devised.

The scheme presented in this paper is based on the wave propagation method of LeVeque [4]. This method is a high-resolution upwind scheme that uses normal and transverse Riemann solvers to obtain a multi-dimensional update. If the divergence-free

constraint is ignored, this method could be used without modification to solve the SMHD equations. In this case, all variables are held at grid cell centers and an approximately non-oscillatory update is guaranteed by the *total variation diminishing* (TVD) nature of the method. This, however, allows for the generation of a non-zero divergence of the magnetic field, which in turn, produces unphysical solutions that can cause the numerical code to crash. A standard approach for correcting this problem is to first use the base scheme to predict a value for the magnetic field ( $\mathbf{B}^*$ ). This value can then be written as

$$h\mathbf{B}^* = \nabla \times \mathbf{A} + \nabla\phi \quad (5)$$

via the Hodge decomposition. By solving the elliptic equation

$$\nabla^2\phi = \nabla \cdot (h\mathbf{B}^*) , \quad (6)$$

the predicted value of the magnetic field can be corrected and made divergence-free:

$$h\mathbf{B}^{n+1} = h\mathbf{B}^* - \nabla\phi . \quad (7)$$

This approach is known as the *projection method*. Because an elliptic solve is required for each time step, this approach is expensive when compared to the base scheme [8].

An alternative class of methods can be developed by first returning to the SMHD equations in continuous form. The evolution of the magnetic field can be written as

$$\partial_t (h\mathbf{B}) + \nabla \times \Omega = 0 , \quad (8)$$

where  $\Omega = -u_1 B_2 + u_2 B_1$  is the electric field. Taking the divergence of both sides of this equation shows that

$$\partial_t [\nabla \cdot (h\mathbf{B})] = 0 ; \quad (9)$$

and therefore, if the magnetic field is initially divergence-free, it will remain so for all time. The base scheme does not satisfy this property because the discrete differential operators do not satisfy the property  $\nabla \cdot [\nabla \times \Omega] = 0$ . A class of schemes known collectively as the *constrained transport* methods have been developed in which the discrete operators are defined such that they mimic their continuous counterparts [8]. In these methods, only the height and the velocities are defined at cell centers. The magnetic field is staggered so that the 1-component sits at left and right cell edges, while the 2-component sits at top and bottom cell edges. A magnetic potential given by  $\nabla \times A = h\mathbf{B}$  is defined at cell corners. To update the solution, a modified Riemann problem based on the SMHD equations is solved to compute new values of the height and velocity field. To update the magnetic potential, a Hamilton-Jacobi equation of the form

$$\partial_t A + \Omega = 0 \quad (10)$$

is solved. New magnetic field values are obtained by differencing this potential. The difficulty of this approach lies in obtaining an appropriate value for the electric field  $\Omega$ . Currently, four distinct approaches exist in the literature [1, 2, 5, 6]. In this paper, these four approaches are compared and a new method based on solving the Hamilton-Jacobi equation via wave propagation methods is developed.

In summary, a new high-resolution wave propagation method for the SMHD equations is presented that utilizes the constrained transport technique to keep the magnetic field divergence-free. Cell centered variables are updated by solving Riemann problems based on the SMHD equations, while staggered magnetic field values are updated by first computing a magnetic potential. In particular, a wave propagation method is developed for solving the Hamilton-Jacobi equation that is satisfied by the magnetic potential. The staggered grid representation of the magnetic field guarantees that the divergence-free constraint is satisfied to machine precision. Furthermore, solutions will remain non-oscillatory near discontinuities since all updates are based on the TVD wave propagation method.

## References

- [1] D.S. Balsara and D. Spicer. A staggered mesh algorithm using high order Godunov fluxes to ensure solenoidal magnetic fields in magnetohydrodynamic simulations. *J. Comp. Phys.*, 149(2):270-292, 1999.
- [2] W. Dai and P.R. Woodward. A simple finite difference scheme for multidimensional magnetohydrodynamic equations. *J. Comp. Phys.*, 142(2):331-369, 1998.

- [3] P.A. Gilman. Magnetohydrodynamic "shallow water" equations for the solar tachocline. *Astrophys. J.*, 544:L79-L82, 2000.
- [4] R.J. LeVeque. Wave propagation algorithm for multi-dimensional hyperbolic systems. *J. Comp. Phys.*, 131:327-335, 1997.
- [5] P. Londrillo and L. Del Zanna. High-order upwind schemes for multidimensional magnetohydrodynamics. *Astrophys. J.*, 530:508-524, 2000.
- [6] D.S. Ryu, F. Miniati, T.W. Jones, and A. Frank. A divergence-free upwind code for multidimensional magnetohydrodynamic flows. *Astrophys. J.*, 509(1):244-255, 1998.
- [7] H. De Sterck. Hyperbolic theory of the "shallow water" magnetohydrodynamics equations. *Physics of Plasmas*, 8(7):3293-3304, 2001.
- [8] Gábor Tóth. The  $\nabla \cdot B = 0$  constraint in shock-capturing magnetohydrodynamics codes. *J. Comp. Phys.*, 161:605-652, 2000.

### **Magnetoplasmdynamic rocket propulsion: Conservation equations and Finite Volume solutions**

Jörg Heiermann\* and Monika Auweter-Kurtz

*Institut für Raumfahrtsysteme, Universität Stuttgart, Germany*

Magnetoplasmdynamic (MPD) rocket propulsion [1, 2] is one option for flying to Mars or to Jupiter's moons in a short time. MPD thrusters typically deliver a thrust up to the 100 N level and a high specific impulse. MPD thrusters use an arc discharge between an anode and a cathode to heat a gas up to more than 10,000 Kelvin. In these axisymmetric devices, the resulting plasma carries an electric current which induces an azimuthal magnetic field. The plasma is thermally expanded and also accelerated by electromagnetic forces, and thus a very high exhaust velocity for efficiently propelling spacecraft is achieved.

Theoretical and numerical investigations have been performed at the Institut für Raumfahrtsysteme (IRS) in order to gain a more profound understanding of the complex physical processes involved [3, 5, 4, 6, 7]. In the IRS laboratory MPD thrusters are investigated experimentally and the numerical and experimental results are compared in order to optimize the thrusters with respect to specific impulse, efficiency, reliability and cost.

An advanced numerical finite volume (FV) code has been written to solve the flow equations very accurately. The argon plasma flow considered is described by conservation equations for species densities, momentum and energy for the heavy particles (atoms and ions), by the conservation equation for electron energy and by the Maxwell equations of classical electrodynamics reformulated as one conservation equation for the magnetic field. Reaction non-equilibrium, thermal non-equilibrium (two-fluid model) and turbulent flow (one-equation model) are assumed.

13 time-dependent conservation equations and some 150 additional constitutive algebraic equations (for example, for the transport properties) must be solved.

The conservation equations are hyperbolic-parabolic and include strong source terms.

For all of the above conservation equations, an advanced second-order accurate finite volume code on adaptive, unstructured meshes with dual cells has been developed. The code includes features like non-linear weighted essentially non-oscillatory (WENO) reconstruction, upwinding with respect to the magnetoacoustic wave and chaotic local time stepping for convergence acceleration. Because only the mass flow is known from the experiment, on the inflow boundary, a numerical mass flow controller solves the Riemann problems between a prescribed inflow state and the inner state at the inflow face. With a constant temperature and a parabolic velocity profile, the pressure of the inflow state is varied until the solution of the Riemann problems delivers the required mass flux. Adaptive mesh refinement is performed using an extension of an asymptotically exact

error estimator for the inviscid Euler equations. The indicator leads to reasonable refinement of boundary layers with extreme gradients at the electrodes, of areas with strong source terms in the nozzle throat, and of shocks.

The conservation equations and the constitutive physical relations as well as the FV discretization are to be presented in detail in this article.

This work is being supported by the German Research Foundation DFG (Deutsche Forschungsgemeinschaft) through the project “Conservation Equations and Numerical Solutions for Technically Relevant Magneto-Plasmas” (Au 85/9-1,2,3), which belongs to the German Priority Research Program (Schwerpunktprogramm) “Analysis and Numerics for Conservation Laws”.

## References

- [1] Jahn, R.G.: Physics of Electric Propulsion, McGraw-Hill Series in Missile and Space Technology, 1968
- [2] Auweter-Kurtz, M.: Lichtbogenantriebe für Weltraumaufgaben, B.G. Teubner Stuttgart, 1992
- [3] Schrade, H.O., Sleziona, P.C., Wegmann, T., Kurtz, H.L.: Basic Processes of Plasma Propulsion, Report grant AFOSR-91-0118, Institute of Space Systems, Stuttgart University, 1992
- [4] Sleziona, P.C.: High Enthalpy Flows for Spaceflight Applications (in German), Habilitation, Aerospace Faculty, Stuttgart University, Germany, 1998
- [5] Wagner, H.P., Kaeppler, H.J., Auweter-Kurtz, M.: Instabilities in MPD thruster flows: 2. Investigation of drift and gradient driven instabilities using multi-fluid plasma models, J. Phys. D: Appl. Phys. 31, pp. 529–541, 1998
- [6] Boie, C.: Numerical Simulation of Magnetoplasma-dynamic Self-field Thrusters with high resolution adaptive schemes, PhD. thesis, Institute of Space Systems, Stuttgart University, Germany, 1999
- [7] Heiermann, J., Auweter-Kurtz, M.: Numerical and Experimental Investigation of the Current Distribution in Self-Field MPD Thrusters, AIAA 2001-3498, 37th AIAA/ASME/SAE/ASEE Joint Propulsion Conference and Exhibit, July 8–11, 2001, Salt Lake City, UT, 2001

### Physical symmetries and hyperbolic divergence correction scheme for Maxwell and MHD equations

Y. J. Lee\*, F. Kemm and C.-D. Munz

*Institut für Aerodynamik und Gasdynamik, Universität Stuttgart, Germany*

One of the important properties of the solutions of Maxwell equations is the conservation of the electric and magnetic charges. But, these charge conservation laws are not strictly obeyed by numerical solutions of Maxwell equations, due to the presence of various types of numerical errors. The violation of the conservation laws is a consequence of the *broken* gauge symmetry in the computational space, which can be recovered by an introduction of the physically consistent counter terms. In this talk, we present a new numerical scheme for the correction of the divergence errors for Maxwell- and MHD equations, which is consistent with the symmetries of Maxwell theory, namely the Lorentz-, gauge- and duality symmetries. The central idea of our divergence correction scheme is the implementation of the physically consistent counter term Ansätze to Maxwell and MHD equations, for the restoration of the gauge symmetry. One of the main advantages of our method is that the divergence conditions for the charge conservations are implemented into the Maxwell and MHD equations in the *hyperbolic* form, rather than the genuine elliptic form, and it can be easily implemented into the existing codes for Maxwell and MHD solvers via operator splitting Ansatz.

## 4.11 Monday, Session 6 (morning): Applications I

### Asymptotic Analysis of Phase-Field Models of Solidification

S. I. Hariharan\*, Curtis Clemons and G. W. Young

*Division of Applied Mathematics, The University of Akron, Akron, OH 44312*

In this talk we study phase-field models related to solidification problems. We consider both pure material systems as well as binary alloy systems. The purpose of this work is to provide an analytic approach to investigate phase-field models. Model parameters are chosen so that the pointwise solutions of the phase-field models agree with the corresponding sharp-interface problems. The analysis presented here is based upon asymptotics in terms of two small parameters: one involving latent heat and another involving the thickness of the interfacial region.

### Solvability and Asymptotic of solutions of Crack-Type Boundary-Contact Dynamic Problems of Elasticity

Otar Chkadua

*A. Razmadze Mathematical Institute, Academy of Sciences of Georgia*

Boundary-contact dynamic problems of elasticity theory are investigated for anisotropic homogeneous media (with contact on some part of the boundary) with cracks. Let  $D_1$  and  $D_2$  finite domains in the  $n$ -dimensional Euclidean space  $R^n$ ,  $n \geq 2$  with the boundaries  $\partial D_q$ ,  $q = 1, 2$ ,  $\partial D_q \in C^\infty$ ;  $D_1 \cap D_2 = \emptyset$ ,  $\partial D_2 = S \cup \partial D_1$ ;  $S \cap \partial D_1 = \emptyset$ ,  $\partial D_1 = S_1 \cup \overline{S_0}$ ,  $S_1 \cap S_0 = \emptyset$ ,  $\partial S_0 = \partial S_1 \in C^\infty$ , where  $S_1$  is the crack surface and  $S_0$  is the contact surface. Suppose that domains  $D_q$ ,  $q = 1, 2$  are filled with different anisotropic homogeneous elastic materials. The basic dynamic equations of elasticity for anisotropic homogeneous elastic media are written as

$$A^{(q)}(\partial_x)u^{(q)}(x, t) - \frac{\partial^2 u^{(q)}(x, t)}{\partial t^2} = F^{(q)}(x, t) \text{ in } D_q \times [0, +\infty[, \quad q = 1, 2,$$

where  $u^{(q)} = (u_1^{(q)}, \dots, u_n^{(q)})$  is the displacement vector,  $F^{(q)} = (F_1^{(q)}, \dots, F_n^{(q)})$  is the mass force to  $D_q$  and  $A^{(q)}(\partial_x)$  is the matrix differential operator

$$A^{(q)}(\partial_x) = \|A_{jk}^{(q)}(\partial_x)\|_{n \times n}, \quad A_{jk}^{(q)}(\partial_x) = a_{ijkl}^{(q)} \partial_i \partial_l, \quad \partial_i = \frac{\partial}{\partial x_i}, \quad q = 1, 2,$$

$a_{ijkl}^{(q)}$  are the elastic constants satisfying the conditions

$$a_{ijkl}^{(q)} = a_{lkij}^{(q)} = a_{ijlk}^{(q)}.$$

under repeated indexes we understand the summation from 1 to  $n$ . It is assumed that the quadratic forms

$$a_{ijkl}^{(q)} \xi_j \xi_l, \quad \xi_j = \xi_{ji}, \quad q = 1, 2$$

with respect to variables  $\xi_{ij}$  are positive definite. We introduce the differential stress operator

$$T^{(q)} = T^{(q)}(\partial_y, n(y)) = \|T_{jk}^{(q)}(\partial_y, n(y))\|_{n \times n}, \quad T_{jk}^{(q)}(\partial_y, n(y)) = a_{ijkl}^{(q)} n_i(y) \partial_l, \quad q = 1, 2,$$

$n(y) = (n_1(y), \dots, n_n(y))$  is the unit normal of the manifold  $\partial D_1 \cup \partial D_2$  at the point  $y \in \partial D_1$  (external with respect to  $D_1$ ) and at the point  $y \in \partial D_2$  (internal with respect to  $D_2$ ). Let  $B$  be some Banach space,  $a > 0$ ,  $m \in \mathbb{N} \cup \{0\}$ . Let  $\mathring{C}_a^m([0, +\infty[, B)$  denote the set of all  $m$ -times continuously differentiable on  $[0, +\infty[$  in  $B$ -valued functions satisfied the conditions:

$$\frac{\partial^l u(0)}{\partial t^l} = 0, \quad l = 0, \dots, m, \quad \left\| \frac{\partial^l u(t)}{\partial t^l} \right\|_B = O(e^{\alpha t}) \quad \forall \alpha > a, \quad l = 0, \dots, m.$$

Define  $C_{0,a}^m([0, +\infty[, B)$  as the set of all  $m$ -times continuously differentiable on  $[0, +\infty[$  in  $B$ -valued functions satisfying the conditions:

$$\frac{\partial^l u(0)}{\partial t^l} = 0, \quad l = 0, \dots, m - 2, \quad \left\| \frac{\partial^l u(t)}{\partial t^l} \right\|_B = O(e^{\alpha t}), \quad l = 0, \dots, m.$$

We have studied the solvability and asymptotics of solutions of the following boundary-contact dynamic problems in the spaces  $C_a^m([0, +\infty[, W_p^1(D_q))$ ,  $q = 1, 2$ :

**Boundary-contact dynamic problem with the Neumann boundary conditions:**

$$\begin{cases} A^{(q)}(\partial_x)u^{(q)}(x, t) - \frac{\partial^2 u^{(q)}(x, t)}{\partial t^2} = F^{(q)}(x, t), & (x, t) \in D_q \times [0, +\infty[, \quad q = 1, 2, \\ \{T^{(2)}u^{(2)}(y, t)\}^+ = \varphi(y, t), & (y, t) \in S \times [0, +\infty[, \\ \{T^{(q)}u^{(q)}(y, t)\}^+ = \varphi_q(y, t), & (y, t) \in S_1 \times [0, +\infty[, \\ \{u^{(1)}(y, t)\}^+ - \{u^{(2)}(y, t)\}^+ = g(y, t), & (y, t) \in S_0 \times [0, +\infty[, \\ \{T^{(1)}u^{(1)}(y, t)\}^+ - \{T^{(2)}u^{(2)}(y, t)\}^+ = f(y, t), & (y, t) \in S_0 \times [0, +\infty[, \\ u^{(q)}(x, 0) = \frac{\partial u^{(q)}(x, 0)}{\partial t} = 0, & x \in D_q, \quad q = 1, 2, \end{cases}$$

where  $F^{(q)} \in C_{0,a}^M([0, +\infty[, L_p(D_q))$ ,  $q = 1, 2$ ,  $\varphi \in C_{0,a}^M([0, +\infty[, B_{p,p}^{-1/p}(S))$ ,  $\varphi_q \in C_{0,a}^M([0, +\infty[, B_{p,p}^{-1/p}(S_q))$ ,  $q = 1, 2$ ,  $g \in C_{0,a}^M([0, +\infty[, B_{p,p'}^{1/p'}(S_0))$ ,  $f \in C_{0,a}^M([0, +\infty[, B_{p,p'}^{-1/p'}(S_0))$ ,  $p' = p/(p - 1)$ ,  $1 < p < \infty$ ,  $M > m + 4$ .

**Boundary-contact dynamic problem with mixed boundary conditions:**

$$\begin{cases} A^{(q)}(\partial_x)u^{(q)}(x, t) - \frac{\partial^2 u^{(q)}(x, t)}{\partial t^2} = F^{(q)}(x, t), & (x, t) \in D_q \times [0, +\infty[, \quad q = 1, 2, \\ \{T^{(2)}u^{(2)}(y, t)\}^+ = \varphi(y, t), & (y, t) \in S \times [0, +\infty[, \\ \{u^{(1)}(y, t)\}^+ = \varphi_1(y, t), & (y, t) \in S_1 \times [0, +\infty[, \\ \{T^{(2)}u^{(2)}(y, t)\}^+ = \varphi_2(y, t), & (y, t) \in S_1 \times [0, +\infty[, \\ \{u^{(1)}(y, t)\}^+ - \{u^{(2)}(y, t)\}^+ = g(y, t), & (y, t) \in S_0 \times [0, +\infty[, \\ \{T^{(1)}u^{(1)}(y, t)\}^+ - \{T^{(2)}u^{(2)}(y, t)\}^+ = f(y, t), & (y, t) \in S_0 \times [0, +\infty[, \\ u^{(q)}(x, 0) = \frac{\partial u^{(q)}(x, 0)}{\partial t} = 0, & x \in D_q, \quad q = 1, 2, \end{cases}$$

where  $F^{(q)} \in C_{0,a}^M([0, +\infty[, L_p(D_q))$ ,  $q = 1, 2$ ,  $\varphi \in C_{0,a}^M([0, +\infty[, B_{p,p}^{-1/p}(S))$ ,  $\varphi_1 \in C_{0,a}^M([0, +\infty[, B_{p,p'}^{1/p'}(S_1))$ ,  $\varphi_2 \in C_{0,a}^M([0, +\infty[, B_{p,p}^{-1/p}(S_1))$ ,  $g \in C_{0,a}^M([0, +\infty[, B_{p,p'}^{1/p'}(S_0))$ ,  $f \in C_{0,a}^M([0, +\infty[, B_{p,p}^{-1/p}(S_0))$ ,  $p' = p/(p - 1)$ ,  $1 < p < \infty$ ,  $M > m + 4$ . Theorems on the existence and uniqueness of solutions of the considered boundary-contact dynamic problems in the spaces  $\mathring{C}_a^m([0, +\infty[, W_p^1(D_q))$  are obtained by using the Laplace transform, the potential theory and the general theory of pseudodifferential equations on a manifold with boundary. Here  $4/3 < p < 4$  in the case of the boundary-contact problem with the Neumann boundary conditions, and  $4/3 < \alpha < p < \beta < 4$  in the case of the boundary-contact problem with mixed boundary conditions where  $\alpha, \beta$  depend on the elastic constants as well as on the geometry of the contact boundary (the crack boundary). A complete asymptotic of solutions is established in the near the contact boundary (the crack end). The properties of exponents of the first terms of asymptotic expansion of solutions are studied and effective formulas for their calculation are found. In particular, the exponent of the first term of asymptotic expansion of solutions of boundary-contact problem with Neumann boundary conditions has the form  $1/2 + i\delta$ . Necessary and sufficient conditions for the vanishing of oscillation are found ( $\delta = 0$ ). Hence the asymptotic expansion of solutions describes a real physical process. In this asymptotic expansion step is one. Further, the asymptotics of solutions of boundary-contact problems with mixed boundary conditions has different properties as compared with the asymptotics of solutions of other problems, i.e.,

1) the real part  $\gamma$  of the exponent of the first term of asymptotic expansion of solutions depend on elastic constants and also on the geometry of the crack boundary, and may take any values from the interval  $]0, 1/2[$ ; a) if the elastic constants satisfy the limit conditions

$$a_{ijkl}^{(2)} / a_{ijkl}^{(1)} \rightarrow 0, \quad \text{then } \gamma \rightarrow 1/2;$$

b) if  $a_{ijkl}^{(2)} / a_{ijkl}^{(1)} \rightarrow \infty$ , then  $\gamma \rightarrow 0$ ;

**2)** classes of isotropic (with elastic constants  $\mu_q, \lambda_q$ ) and also transversally-isotropic (with elastic constants  $c_{11}^{(q)}, c_{33}^{(q)}, c_{13}^{(q)}, c_{55}^{(q)}, c_{66}^{(q)}$  in the conditions  $c_{11}^{(q)} = c_{33}^{(q)}$ ) bodies are found for spatial ( $n = 3$ ) boundary-contact problems with mixed boundary conditions when oscillation vanishes in the asymptotic expansion of solutions. In such cases, effective formulas are obtained for calculating exponents of the first terms of the asymptotics:

$$\gamma = \frac{1}{2} - \frac{1}{\pi} \operatorname{arctg} \sqrt{\frac{\mu_2}{\mu_1}} \quad (\text{the isotropic case})$$

and

$$\gamma = \frac{1}{2} - \frac{1}{\pi} \operatorname{arctg} \sqrt[4]{\frac{c_{55}^{(2)} c_{66}^{(2)}}{c_{55}^{(1)} c_{66}^{(1)}}} \quad (\text{the transversally-isotropic case}).$$

Note that the first terms have no logarithms. I'd like to note, that these classes are found only in spatial problems since it is known that in such cases oscillation does not vanish in plane problems. In the transversally-isotropic case we assume that the neighborhood of the contact boundary is parallel to the isotropic plane.

**3)** in the general case (in particular, in the transversally-isotropic case, where  $c_{11}^{(q)} \neq c_{33}^{(q)}, q = 1, 2$ ) we have found a class of anisotropic bodies when the oscillation in the expansion vanishes, while the real part  $\gamma$  of the exponents of the first term of the asymptotic expansion is calculated by a simpler formula

$$\gamma = \frac{1}{2} - \sup_{1 \leq j \leq n} \frac{1}{\pi} \operatorname{arctg} \frac{1}{\sqrt{\alpha_j \beta_j}},$$

where  $\alpha_j > 0, \beta_j > 0$  ( $j = 1, \dots, n$ ) are eigenvalues of the principal homogeneous symbols of the Poincaré–Steklov operators.

**4)** if the domains are filled with the same material, then the exponents of the first and second terms have the form  $1/4 + i\delta_1, 3/4 + i\delta_2$  respectively; these terms are free from logarithms and oscillation does not vanish. In this asymptotic expansion step is one-half. The time parameter  $t$  in asymptotic expansion of solutions participates only in coefficients. In some particular cases of spatial dynamic boundary-contact problems with cracks of half-plane type, the first coefficient of solutions of asymptotics is calculated, which depends on elastic constants, the time parameter  $t$  and global boundary and boundary-contact values. In these cases, the so-called Griffiths criterion can be formulated as problem of finding a moment of time after which the crack begins to grow.

## 4.12 Monday, Session 6 (afternoon): Applications II

### Simulation of the motion and heating of an irregular plasma

V. T. Astrelin and A. V. Burdakov

*Institute of Nuclear Physics, Siberian Division, Russian Academy of Sciences, Novosibirsk 630090, Russia*

N. A. Huber\*

*Novosibirsk State University, Novosibirsk 630090, Russia*

V. M. Kovenya

*Institute of Computational Technologies, Siberian Division, Russian Academy of Sciences, Novosibirsk 630090, Russia*

In recent decades, plasma heating and confinement has become an important problem in plasma physics. Because of the variety of regimes, the wide range of parameters of the medium, and the complexity and nonlinearity of the examined processes, problem of plasma heating and propagation is a multiparameter one, which requires using various approaches to solve it. In the present work, a numerical simulation of the plasma dynamics is used in experiments on heating and motion of a dense gas cloud. The expansion of a plasma cloud in an external magnetic field is studied using some simplifications in a magnetohydrodynamic approximation. The basic equations include continuity, motion, energy and magnetic-field equations. For numerical solution of the problem, a finite-difference scheme of the type of a universal algorithm with splitting into physical processes and spatial directions is developed, which allowed to obtain separate solutions of the equations of magnetic induction and gas dynamics. Calculations of the propagation of a plasma cloud heated by a source in an external magnetic field were performed. The mechanism of the effect of the magnetic field and heat source on plasma cloud expansion is determined.

### Wave Processes Of Collapsing Bubbles Containing Generic Or Retrograde Gases

Sigrid Andreae\* and Josef Ballmann

*Lehr- und Forschungsgebiet für Mechanik der RWTH Aachen, Germany*

The process of production of cavities or bubbles in a liquid is called cavitation. It is caused by a pressure drop in the liquid below vapor pressure. This may occur in the flow of a liquid through a narrow orifice or around an obstacle. In flow regions with pressure above vapor pressure the bubbles will collapse. This collapse is accompanied by strong shock and rarefaction waves. Their damaging effect on solids is observed in experiments [4]. However, the prediction of onset and extent of the cavitation damaging is not satisfying. Up to now little is known about the physical processes taking place in the interior of the collapsing bubble [3]. Small time and space scales make an experimental approach difficult. The numerical investigations are expected to reveal information about the physics inside the bubble and the damaging of the solid. In addition, the possibility is included that the cavitating fluid may be not generic but a BZT (Bethe-Zel'dovich-Thompson) fluid. This is of importance since some liquid fuels belong to that group. Normally, a collapsing gas bubble in a liquid is modeled as a two phase flow problem. In that case one has to treat the gas-liquid boundary, either tracing it with a method like level-set or volume of fluid or using two meshes in order to distinguish between the two phases. At least the second case is numerically very expensive since the mesh has to be updated in every step. To overcome that problem we model the gas as well as the liquid with the same equation of state. We choose the van der Waals equation of state (thermal: eq. 1, caloric: eq. 2) since it yields qualitative good results for the gas as well as for the liquid phase,

$$p(v, T) = \frac{RT}{e(v, T) - b} - \frac{a}{v^2} \quad (1)$$

$$e(v, T) = \epsilon_0 + b c_v \left( \frac{T}{v} \right) T - \frac{a}{v} \quad (2)$$

|        |                         |       |                 |
|--------|-------------------------|-------|-----------------|
| $p$    | pressure                | $T$   | temperature     |
| $e$    | internal energy         | $v$   | specific volume |
| $R$    | specific gas constant   | $c_v$ | heat capacity   |
| $a, b$ | van der Waals constants | $s$   | entropie        |

Besides it provides a proper representation for BZT Fluids. In the single phase regions the only parameter of the equation that changes is the heat capacity which has to be implemented as a function of temperature and specific volume,

$$c_v(v, T) = c_v^0 + T \int \left( \frac{\partial^2 p}{\partial T^2} \right)_v dv. \quad (3)$$

However, the van der Waals equation can not be used in the region of phase transition since it shows an unphysical inclination in the  $p$ - $v$ -diagram. Between the two spinodal points at the end of the supersaturated vapor and overexpanded liquid curve the first derivative of  $p$  by  $v$  is positiv which is thermally unstable. In this region pressure as a function of volume and temperature has to be calculated by means of the maxwell construction. It is implemented using a numerical library for equations of state written at the IGPM by A. Voß [6].

BZT Fluids are high molecular hydrocarbons or -fluorids. They are a subgroup of retrograde fluids which exhibit a characteristic overhang of the wet steam curve in the  $T$ - $s$ -diagram. Near that hat-sphaped overhang they can condense on isentropic compression. The overhang leads to a concave bending of the isentropes near the critical point in the  $p$ - $v$ -plane. This is in contrast to generic fluids whose isentropes are convex. A measure for that bending is the fundamental derivative,  $\Gamma$ , which becomes negative in that region.

$$\Gamma = \frac{v^3}{2c^2} \frac{\partial^2 p}{\partial v^2}, \quad c^2 = \left. \frac{\partial p}{\partial \left(\frac{1}{v}\right)} \right|_s \quad (4)$$

The gasdynamic curiosity of the  $\Gamma < 0$ -region is the possibility of expansion shocks. To fulfill the entropy condition across a shock in case of a negative fundamental derivative the pressure jump has to be positive. The closure of the system of conservation laws requires caloric and thermal equations of state which are able to describe these effects properly. The chosen van der Waals equation of state provides a good representation of the effects in the region of negative  $\Gamma$ .

The fluid is modeled by the time-dependent Navier-Stokes equations for compressible fluid flows. Neglecting effects of viscosity and heat conduction, the system is hyperbolic, otherwise parabolic. The system is solved using an implicit Finite Volume scheme on structured grids based on Roe's approximate Riemann solver [5] in a formulation by Grotowsky [1] for two-dimensional flows, extended by Hanke [2] for flows with rotational symmetry.

As test case a hot gas bubble at low pressure surrounded by the same gas at high pressure and low temperature was computed with a perfect gas equation. First the case of a bubble in a free fluid with no solid boundaries is investigated, see fig. 1. The results of the single phase simulation are encouraging. The shock wave running into the bubble's center as well as the following contact discontinuity are well resolved. Due to the rotational symmetry the focusing shock wave reinforces and is reflected in the center. Afterwards it crosses the contact discontinuity and evokes thereby Rayleigh Taylor fingering instabilities. The next test case is to place the bubble near a solid wall. The results which show a liquid jet towards the wall will be presented. This permits an evaluation of the walls influence on the collapse process. The results which show a liquid jet towards the wall will be presented. Then the same cases will be investigated for the van der Waals equation of state for a generic as well as for a BZT fluid.

## References

- [1] I.M.G. Grotowsky. *Ein numerischer Algorithmus zur Lösung der Navier-Stokes-Gleichungen bei Über- und Hyperschall-machzahlen*. PhD thesis, RWTH Aachen, VDI-Verlag, Reihe 20, Nr. 145, 1994.
- [2] M. Hanke. *Die Navier-Stokes-Gleichungen in krummlinigen Koordinaten; Diskretisierung für Upwind-Schemata*. Lehr- und Forschungsgebiet für Mechanik, RWTH Aachen (unpublished), 1995.
- [3] M. Hanke. *Analyse und Bewertung physikalischer Modelle fr große Zustandsänderungen in kollabierenden Blasen*. Diplomarbeit, Lehr- und Forschungsgebiet für Mechanik, RWTH Aachen, 1997.
- [4] A. Philipp and W. Lauterborn. Cavitation Erosion By Single Laser-produced Bubbles. *J. Fluid Mech.*, 361:75–116, 1998.

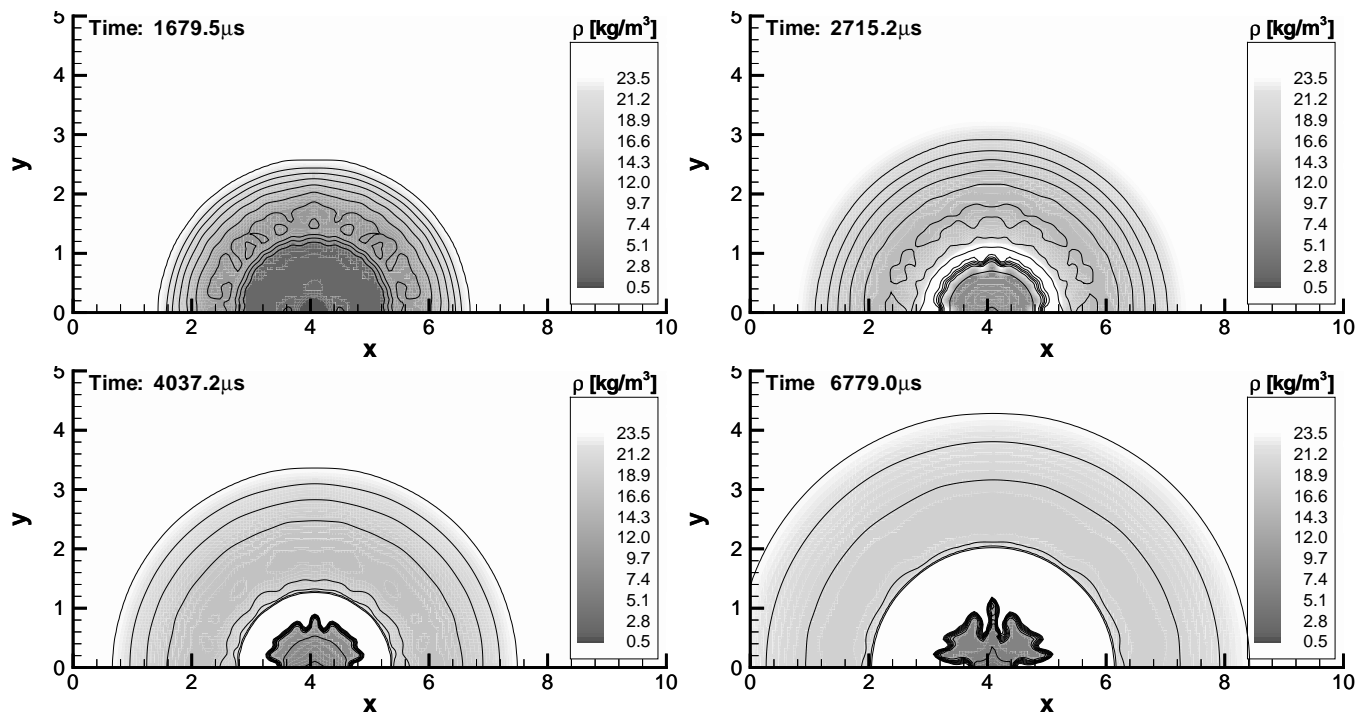


Figure 1: I.C. interior:  $p = 1\text{bar}$ ,  $T = 693\text{K}$ ; I.C. exterior:  $p = 20\text{bar}$ ,  $T = 293\text{K}$

- [5] P.L. Roe. Approximate Riemann Solvers, Parameter Vectors, And Difference Schemes. *J. Comput. Phys.*, 43:357–372, 1981.
- [6] A. Voß. A Numerical Library For Fluids And Convex And Nonconvex EOS Considering Phase Transitions. *IGPM-report*, RWTH Aachen, 2002, in preparation.

### The Flow of Thin Liquid Films with a Contact Line

Michael Shearer

*CRSC and Mathematics Department, North Carolina State University*

A fourth order nonlinear pde describes the flow of a thin liquid film up an inclined surface, under opposing forces of gravity and shear stress. The Navier slip condition allows a small amount of slip between the liquid and the solid surface near the contact line; it is designed to remove the stress singularity that occurs under the usual no-slip condition. Numerical solutions reveal a subtle connection between the contact line dynamics and the nonlinear transport represented by the underlying nonconvex scalar conservation law. In particular, traveling waves are identified as compressive or undercompressive, depending on whether upstream characteristics enter or leave the contact line. The results include asymptotics at the contact line, and the analysis of an associated planar vector field.

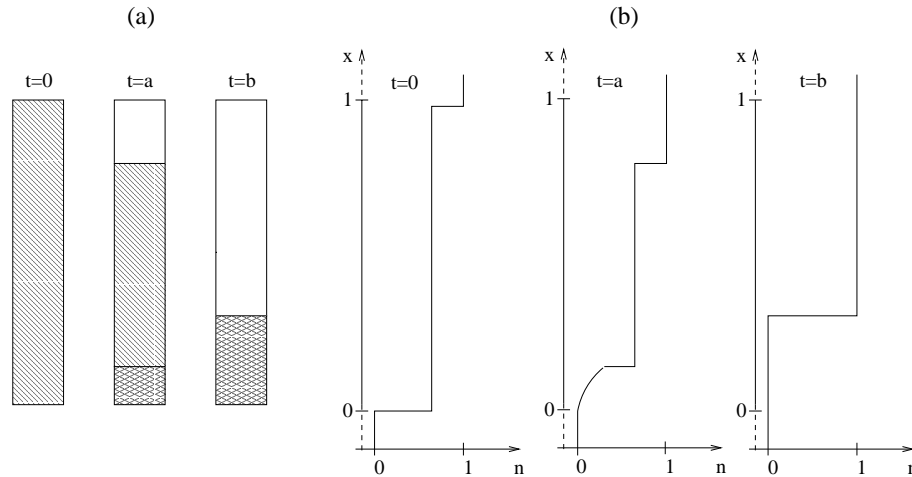


Figure 1: (a) Schematic diagram of a soil sedimentation experiment in a settling column. Initially ( $t = 0$ ) the whole column is filled with a soil-water suspension with uniform porosity  $n$ . (b) The nonlinear wave phenomena in settling column experiments modelled by a scalar conservation law.

### Nonconvex Flux Functions and Compound Shock Waves in Sediment Beds

Gert Bartholomeeusen\*

*University of Oxford, UK*

Hans De Sterck

*University of Colorado at Boulder, USA*

Gilliane C. Sills

*University of Oxford, UK*

Sediment layers deposited under water undergo a deformation that for low soil concentrations can be described by a scalar nonlinear hyperbolic conservation law. The associated flux function is nonconvex and compound shock waves, which are shocks followed or preceded by a sonic rarefaction, arise. The paper describes an experimental study of compound shock waves in sediment beds and the numerical modelling of the sedimentation process using an experimentally obtained flux function for kaolinite soil. The non-convexity of the flux function is investigated as it is quite different from what usually is assumed for soil suspensions. The work also fits in a broader investigation of the transition parameter between the physical processes of soil sedimentation and consolidation, as the data obtained allows identification of this parameter.

Fig. 1(a) shows a schematic diagram of a soil sedimentation experiment in a settling column. Initially ( $t = 0$ ) the whole column is filled with a soil-water suspension with uniform porosity  $n$ , defined as the volume of voids divided by the total volume. During the subsequent temporal evolution (middle panel), nonlinear wave fronts propagate from the top and bottom of the column into the suspension. A sediment-water interface propagates downward from the top surface, separating a top layer consisting of pure water from a middle layer which has the initial porosity. The porosity changes in an almost discontinuous or shock-like fashion over the sediment-water interface. When initial porosities are not too low, the middle layer is separated from a bottom layer by an upward propagating porosity step, over which the porosity changes discontinuously as well. Detailed measurements of porosity profiles show that this porosity step is followed by a continuous rarefaction wave, which forms, together with the porosity step, a so-called compound shock wave. Compound shocks are wave structures composed of a shock followed or preceded by a rarefaction that is sonic — i.e., the point where the rarefaction is attached to the shock propagates with the local wave speed [6]. It is well-known that compound shocks arise in systems described by hyperbolic conservation

laws with non-convex flux functions, i.e, for which wave speeds do not vary in a monotonous manner with relevant changes of the state variables. Many physical systems that can be described by hyperbolic conservation laws have flux functions with quadratic nonlinearities that are convex. For example, the scalar Burgers equation and the system of Euler equations for gas dynamics are convex such that compound shocks do not occur. More complex flux functions may be obtained when real gases are modelled, which may allow for the occurrence of compound shocks. An early example of a non-convex scalar flux function is given by the Buckley-Leveret equation which models two-phase flows that pertain to oil recovery problems [6]. This equation exhibits a cubic flux function. The system of magnetohydrodynamics equations has two non-convex modes [2] and exhibits compound shocks, which have been found in numerical simulations in one, two and three spatial dimensions [2, 3, 4]. Compound waves and non-convex flux functions for sedimentation processes have been discussed first by Kynch [5], and later also by Wallis [6]. In Fig. 1(b) it is indicated how the nonlinear wave phenomena in settling column experiments can be modelled by a scalar conservation law

$$\frac{\partial n}{\partial t} + \frac{\partial f(n)}{\partial x} = 0, \tag{1}$$

with a non-convex cubic flux function, which allows for the occurrence of compound shocks. The initial condition contains two Riemann problems at  $x = 0$  and  $x = 1$  ( $t = 0$ ). A shock wave propagates downward, and a compound shock propagates upwards ( $t = a$ ).

The goal of the present paper is to produce an appropriate flux function for the kaolinite sedimentation process based on unique experimental data obtained using X-rays. First, it is illustrated how the main features of the nonlinear wave phenomena that occur in settling column sedimentation experiments can be described by a scalar hyperbolic conservation law model with a simple cubic non-convex flux function. Second, extensive experiments are performed on a very-grained Kaolinite soil, which is naturally exploited, but industrially processed for amongst others the paper industry. Sedimentation experiments are performed in 102 mm diameter acrylic columns [1, 7]. Uniformly distributed suspensions are deposited at different initial porosities to study the different forms of shock waves that arise. The surface settlement is monitored of experiments starting at high porosity or low concentration to study the regular shock wave of the water-sediment interface. Fig. 2 shows a selection of experimental results with initial porosities ranging from 0.93 to 0.98. Experiments starting at lower porosity are additionally monitored with an X-ray absorption technique [1]. In these X-ray monitored experiments it is possible to track accurately the porosity step in the sediment bed and study compound shock waves and rarefaction waves. Fig. 3 shows an example of an experimentally observed compound shock wave, which consists of a porosity step followed by a sonic rarefaction wave. Note the clear similarity with the middle profile of Fig. 1(b). The sedimentation behaviour of Kaolinite for high initial porosities will result in a initial constant

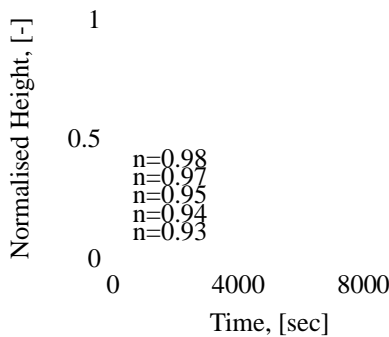


Figure 2: Overview of Surface Settlement Monitoring Kaolinite Experiment with Normalised Height.

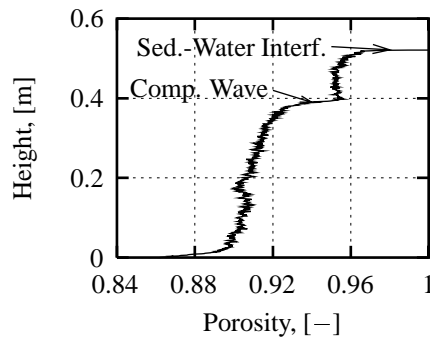


Figure 3: X-ray porosity measurement, Kao2dd, with Shock Tracking.

settling rate as observed in Fig. 2. The porosity just under the shock is still the initial value and a point of the flux curve can thus be calculated. Experiments where the porosity step is tracked with time, Fig. 3, give information about the location of the compound shock wave. Since the sediment layer is a continuum, the velocity of fixed material or Lagrangian coordinates can be calculated from identifying the corresponding Eulerian coordinates of consecutive measurements. Thus X-ray profiles provide the solid's velocity and porosity for consecutive measurements, and the corresponding flux can be derived. In this way the non-convexity of the Kaolinite flux function can be quantified. It is shown that the flux curve of Kaolinite is quite different from what is usually assumed for soil suspensions in terms of the locus and amplitude of the convex extremum.

The unique experimental data leading to an appropriate flux function demonstrate that the experimental method used provides

a flux function that is significantly improved over what has been available. The conference presentation will include video demonstrations of shock wave processes in settling soil.

## References

- [1] BEEN, K., & SILLS, G.C. 1981. Self-weight consolidation of soft soils. *Géotechnique*, **31**, 519–535.
- [2] BRIO, M., & WU, C.C. 1988. An upwind scheme for the equations of ideal magnetohydrodynamics. *Journal of computational physics*, **75**, 400–422.
- [3] DE STERCK, H., LOW, B.C., & POEDTS, S. 1999. Characteristic analysis of a complex two-dimensional magnetohydrodynamic bow shock flow with steady compound shocks. *Physics of plasmas*, **6**(3), 954–969.
- [4] DE STERCK, H., LOW, B.C., & POEDTS, S. in press. Overcompressive shocks and compound shocks in 2D and 3D magnetohydrodynamic flows. In: *Proceedings of the Eighth International Conference on Hyperbolic Problems*.
- [5] KYNCH, G.J. 1952. A theory of sedimentation. *Transactions faraday society*, **48**, 166–176.
- [6] LEVEQUE, R.J. 1992. *Numerical methods for conservation laws*. Birkhäuser Verlag, Basel.
- [7] SILLS, G.C. 1998. Development of structure in sedimenting soils. *Philosophical transactions of the Royal Society of London A*, **356**, 2515–2534.
- [8] WALLIS, G.B. 1969. *One-dimensional two-phase flow*. McGraw-Hill Book Company.

### 4.13 Tuesday, Session 1 (morning): Vanishing viscosity

#### Vanishing viscosity approximation of multidimensional shock and boundary layers

Kevin Zumbrun

*Indiana University, Bloomington, USA*

We present joint work with Olivier Gues, Mark Williams, Guy Métivier; see [MZ, GMWZ]. The basic question under consideration is existence of (noncharacteristic) multidimensional viscous boundary and shock layers in the vanishing viscosity limit: more precisely, validity of matched asymptotic expansions constructed, respectively, in [GG] and [GW]. This problem has been addressed in the one-dimensional case in [GS,GR] (boundary layers) and [GX,Y,R.1] (shocks). In the multidimensional boundary layer case, validity has been established for small amplitude layers and “prepared” (i.e. viscosity-dependent) data in [GG]; important preliminary investigations have been carried out in [R.2] for the large amplitude case. Here, as in [GR,R.1–2], we allow arbitrary amplitude layers for which the inner layer satisfies an appropriate Evans function condition that is necessary for stability. In the case of prepared data, we give a complete analysis; for unprepared data, we indicate the new difficulties involved, and present partial results obtained so far.

The standard strategy in the vanishing viscosity problem (see, e.g., discussion in [GG]) is to: (i) construct an approximate solution to appropriately high order; and (ii) establish linearized stability of the approximation. Step (i) has been carried out in [GG,GW] to arbitrarily high order, at least for the case of prepared data. Thus, our focus here is on stability. (However, note that the two problems are not disjoint, particularly in the case of unprepared data). Away from layers, this may be established in somewhat standard fashion by paradifferential (symmetrizer) techniques. However, the fast “inner layer” of the solution must be treated more carefully.

Detailed  $L^2 \rightarrow L^p$  ( $p \geq 2$ ) linear estimates for planar shock layers have been established in [Z] by direct calculation/resolvent estimates; however, these techniques are not available in the time-varying “curved shock” setting we now consider, nor for the time-varying boundary layer problem. Moreover, we are restricted in multi-dimensions by the hyperbolic (or “outer”) part of the solution to seeking  $L^2 \rightarrow L^2$  bounds, analogous to but (even in the constant-coefficient case) distinct from the  $L^1$  Green’s function bounds found in [GR]. And, we must obtain these bounds by a method suitable for the analysis of both hyperbolic boundary-value problems and their parabolic regularizations.

To satisfy these requirements, we follow Kreiss’ analysis of hyperbolic boundary value equations. Our basic estimates concerns the  $L^2$  stability of the linearized equations, and are proved using symmetrizers and a suitable extension of Kreiss’ analysis to parabolic-hyperbolic problems, and to shock (vs. boundary) layers. It can be seen by comparison with explicit representations of the resolvent in the planar case, carried out respectively in [A] and [Z], that this basic estimate is sharp *for both hyperbolic and parabolic parts of the equations*. Moreover, we significantly relax the structural assumptions under which the parabolic results of [Z] were obtained, just as the Kreiss analysis relaxed the assumptions necessary for the hyperbolic results of [A].

In the shock case, there is an additional difficulty that, as in the hyperbolic case, the boundary conditions induced by considering the problem as a doubled boundary value problem are *singular*, with associated Lopatinski determinant vanishing to the order of the frequency of perturbing signals. In the hyperbolic case [Ma,M], the singularity is confined to a variable describing front location, so does not affect interior estimates. In the hyperbolic–parabolic case under consideration, this “decoupling” is not explicit, and must be detected through the analysis. To overcome this difficulty, we introduce a new class of “degenerate symmetrizers” weighting “parabolic” (fast) modes less than “hyperbolic” (slow) modes. These have the effect to maintain the usual, hyperbolic interior estimates, while giving up trace estimates in the unique singular parabolic mode. This mode, approximately described by the spatial derivative of the front, can be viewed as encoding the shock location, so that the estimates obtained are completely analogous to those of the hyperbolic case.

The basic  $L^2 \rightarrow L^2$  symmetrizer estimates just described are the key results needed to carry out the prepared data bounded time vanishing viscosity problem, which in the shock case roughly corresponds to the artificial problem of long-time asymptotic stability of planar fronts for *zero mass data*. However, it is easily seen that they do not suffice for general data. More precisely, the ordering by strength of needed *planar* estimates is: prepared data vanishing viscosity  $\leq$  zero mass planar stability  $<$  nonzero mass planar stability  $\leq$  unprepared data vanishing viscosity. Using a novel (and rather delicate) duality argument together with the degenerate symmetrizer techniques just described, we are able to obtain also sharp  $L^1 \rightarrow L^2$  bounds sufficient for the treatment of the nonzero mass planar problem. Indeed, we recover the  $L^2$  decay results of [Z], with only slightly stronger assumptions on regularity of initial data (needed to control  $L^\infty$  by Sobolev embedding). So far as we know, this is the first use of symmetrizers to obtain estimates from spaces other than  $L^2$ , which are essential for the nonzero mass case.

Though far from certain, it is our hope that these newer techniques will be of use in treating the unprepared data vanishing viscosity problem that is our ultimate goal. In any case, they give an appealing (and illuminating) alternative proof of long time asymptotic stability in the planar case.

## REFERENCES

- [A] S. Agmon, *Problèmes mixtes pour les équations hyperboliques d'ordre supérieure, Les Équations aux Dérivées Partielles*, Éditions du Centre National de la Recherche Scientifique, Paris (1962) 13–18.
- [GG] E. Grenier and O. Gues, *Boundary layers for viscous perturbations of noncharacteristic quasilinear hyperbolic problems*, J. Differential Equations 143 (1998), no. 1, 110–146.
- [GMWZ] O. Gues, G. Métivier, M. Williams, and K. Zumbrun, *Degenerate symmetrizers and the stability of multidimensional viscous shocks*, in preparation.
- [GR] E. Grenier and F. Rousset, *Stability of one-dimensional boundary layers by using Green's functions*, Comm. Pure Appl. Math. 54 (2001), no. 11, 1343–1385.
- [GW] O. Gues and M. Williams, *Curved shocks as viscous limits: a boundary problem approach*, Preprint (2001).
- [Ma], A. Majda, *The stability of multi-dimensional shock fronts – a new problem for linear hyperbolic equations*, Mem. Amer. Math. Soc. 275 (1983).
- [M] G. Métivier, *Stability of multidimensional shocks*, Birkhauser's Series: Progress in Nonlinear Differential Equations and their Applications (2001), 24–103.
- [MZ] G. Métivier and K. Zumbrun, *Large viscous boundary layers for noncharacteristic nonlinear hyperbolic problems*, preprint (2002).
- [R.1] F. Rousset, *Viscous limits for strong shocks of systems of conservation laws*, preprint (2001).
- [R.2] F. Rousset, *Inviscid boundary conditions and stability of viscous boundary layers*, Asymptot. Anal. 26 (2001), no. 3-4, 285–306.
- [Y] S.-H. Yu, *Zero-dissipation limit of solutions with shocks for systems of hyperbolic conservation laws*, Arch. Ration. Mech. Anal. 146 (1999), no. 4, 275–370.
- [Z] K. Zumbrun, *Multidimensional stability of planar viscous shock waves*, Birkhauser's Series: Progress in Nonlinear Differential Equations and their Applications (2001), 307–516.

### Parabolic problems which are ill-posed in the zero dissipation limit

Jacob Yström\*

*Department of Numerical Analysis and Computer Science KTH Stockholm Sweden*

Heinz-Otto Kreiss

*Department of Mathematics University of California at Los Angeles, USA*

We consider linear second order parabolic Cauchy problems which are ill-posed in the limit of zero dissipation. We show that for smooth coefficients the principle of frozen coefficients is applicable. That is, the growth rate predicted by this principle for a small viscosity parameter is correct. We discuss the limitation of this principle and show by examples that if the coefficients are varying on a scale that is proportional to the viscosity parameter then the problem need not be unstable. For non-linear problems we can conclude that smooth solutions in regions where the characteristics are complex are not stable. We show that small perturbations of smooth complex initial data for the viscous Burgers' equation result in a  $\mathcal{O}(1)$  change of the solution. For two non-linear examples, numerical calculations demonstrate that for smooth initial data the solutions rapidly form non-smooth solutions – dissipative structures – that stabilizes the inherent instabilities.

**Green's function pointwise estimates for the modified Lax-Friedrichs scheme**

Pauline Godillon-Lafitte

UMPA, ENS Lyon, FRANCE

When considering one-dimensional hyperbolic systems of conservation laws

$$\begin{aligned} u_t + f(u)_x &= 0, \\ u : \mathbf{R} \times \mathbf{R}^+ &\rightarrow \mathbf{R}^d, f \in \mathbf{C}^\infty(\mathbf{R}^d), d \geq 2, \end{aligned} \tag{1}$$

with an initial datum  $u(x, 0) = u_0(x)$ ,  $x \in \mathbf{R}$ , a natural way to approximate solutions is to mesh the time and space variables :  $t \sim kn$ ,  $n \in \mathbf{N}$  and  $x \sim hj$ ,  $j \in \mathbf{Z}$ . We are interested here in the non-homogeneous numerical problem associated to the modified Lax-Friedrichs scheme

$$u^{n+1} = \mathcal{N}(u^n), n \geq 1, \text{ and } u_j^0 = u(jh) \tag{2}$$

where the (nonlinear) operator  $\mathcal{N}$  reads

$$(\mathcal{N}u)_j = u_j - (k/h)(\mathcal{F}(u_j, u_{j+1}) - \mathcal{F}(u_{j-1}, u_j)), j \in \mathbf{Z}, \tag{3}$$

the numerical flux  $\mathcal{F}$  being defined  $\mathcal{F}(u, v) = (f(u) + f(v))/2 + \mathbf{D}(u - v)$ , with  $\mathbf{D}$  a scalar constant. Assuming that, given a non-characteristic stationary shock  $(u^-, u^+)$  of (1) such that (1) is strictly hyperbolic at  $u^\pm$ , there exists an associated discrete shock profile  $\bar{u}$  of (3), that is, a fixed point of  $\mathcal{N}$ , we aim here to study the linear stability of  $\bar{u}$  : denoting by  $L$  the linearized operator about  $\bar{u}$ , we consider the non-homogeneous problem

$$v^{n+1} - Lv^n = \tilde{v}, n \geq 1, \tag{4}$$

$$v_j^n \rightarrow 0, j \rightarrow \pm\infty, n \in \mathbf{N}, \tag{5}$$

$$v^0 = v, \tag{6}$$

where  $\tilde{v}$  and  $v$  are given. Given  $l \in \mathbf{Z}$ , the Green's function  $(G(j, n; l))_{(j,n) \in \mathbf{Z} \times \mathbf{N}}$  is a sequence of matrices that satisfies (4)-(5)-(6) with  $\tilde{v} = 0$  and  $v_j = \delta_{jl}$ ,  $\delta$  denoting the Kronecker symbol, so that, thanks to the superposition principle, the solutions of (4)-(5)-(6) can be expressed through  $G$ ,  $\tilde{v}$  and  $v$ .

Following Zumbrun and Howard's work on the viscous approximation [5] and assuming that  $\bar{u}$  is spectrally stable, that is  $L$  has no spectrum outside the disc  $\{|\mu + 1| < 1\}$  except possibly  $\mu = 0$ , we obtain a precise description of the behaviour of the Green's function [3]:

$$G(j, n; l) = \mathbf{O} + \mathbf{E} + R,$$

where  $\mathbf{E}$  corresponds to an excited stationary term, that takes the form of a projection on the kernel of  $L$ ,  $\mathbf{O}$  is a sum of Gaussian-type waves that reads

$$\mathbf{O} = \sum_{q/a_q^\pm j > 0} \frac{1}{\sqrt{n}} O \left( \exp \left( -\frac{(hj - ka_q^\pm n)^2}{Mh^2n} \right) \right) r_q^\pm,$$

with  $a_q^\pm$  the eigenvalues of  $df(u^\pm)$  and  $r_q^\pm$  some corresponding eigenvectors, and  $R$  is a fast-time decaying term.

This result is analogous to the ones proved by Zumbrun and Howard [5] in the case of viscous shock profiles, although they do not set on  $y$  (the continuous analogue of our discrete variable  $l$ ) to be bounded.

Let us now give a physical interpretation of this result. At first, the Dirac mass splits into waves that propagate along the outgoing characteristics and waves that propagate along the entering characteristics. The waves that are carried by the outgoing characteristics, that is eigenvectors corresponding to negative (respectively positive) eigenvalues if the Dirac mass was on the left-hand (resp. right-hand) side of the shock, take the shape of moving Gaussians that are damped by the numerical viscosity. Their asymptotic speeds are the corresponding eigenvalues of the derivatives of the flux at the end states multiplied by the ratio  $k/h$ . The waves propagating along the entering characteristics move towards the shock, and when each wave corresponding to a different characteristic reaches the position of the shock ( $j = 0$ ), similar outgoing waves as described above are emitted. Furthermore, if the shock is compressive, as soon as the first entering waves has reached the shock, a stationary residual wave

that is strongly related to the kernel of  $L$  may appear, depending on the position of the Dirac mass as initial datum. There is also a fast-time decaying term. Note that the fact that the outgoing waves are Gaussian-shaped is compatible with the  $\ell^1$  conservation of the mass.

Numerical simulations are available at <http://www.umpa.ens-lyon.fr/~pgodillon/>.

The main tool that we use is the Laplace transform with respect to  $n$  that is defined by

$$v = (v^n)_{n \in \mathbf{N}} \mapsto \left( \lambda \in \mathbf{D} \mapsto \hat{v}(\lambda) := \sum_{n \in \mathbf{N}} e^{-\lambda n} v^n \right), \quad (7)$$

where  $\mathbf{D}$  is a subset of  $\mathbf{C}$  that we choose such that the sum in (7) converges. In particular, since (7) is  $i2\pi$ -periodic, we set on  $\mathbf{D}$  to be contained in the strip  $\mathcal{S} := \{\lambda \in \mathbf{C} / -\pi \leq \text{Im}(\lambda) \leq \pi\}$ . Given  $l \in \mathbf{Z}$ , the Laplace transform of  $G(\cdot, \cdot; l)$  with respect to  $n$  that we denote by  $G_\lambda(j; l)$  is a solution of the following problem

$$(L - e^\lambda + 1)G_\lambda(j; l) = -\delta_{lj}e^\lambda I_d, \quad j \in \mathbf{Z}, \quad (8)$$

$$G_\lambda(j; l) \rightarrow 0, \quad j \rightarrow \pm\infty. \quad (9)$$

We rewrite the eigenvalue equation  $(L - e^\lambda + 1)v = 0$  associated to  $L$  as a first-order dynamical system

$$V_j = \mathbf{A}_j(\lambda)V_{j-1}, \quad V_j = \begin{pmatrix} v_j \\ v_{j+1} - v_j \end{pmatrix} \in \mathbf{C}^{2d}, \quad j \in \mathbf{Z}. \quad (10)$$

Thanks to the spectral stability assumption,  $\lambda \mapsto G_\lambda(\cdot; l)$  is holomorphic in  $\{\Re(\lambda) > 0\}$ . Besides, we express  $G_\lambda(\cdot; l)$  in a basis  $\mathcal{B}$  (resp.  $\mathcal{C}$ ) of solutions of system (10) that tend to 0 as  $j$  tends to  $+\infty$  (resp. as  $j$  tends to  $-\infty$ ), so that we are able to prove that, thanks to the Gap Lemma of Gardner and Zumbrun [2, 5],  $G_\lambda(\cdot; l)$  is meromorphic in  $\{\Re(\lambda) > -\eta, |\Im(\lambda)| \leq \pi\}$ ,  $\eta$  being positive, with a pole at  $\lambda = 0$  or holomorphic in this neighborhood depending on the nature of the shock. Then we compute estimates of  $G_\lambda$  for bounded  $l$ . Finally, we find estimates of  $G$  thanks to the inverse Laplace transform

$$G(j, n; l) = \frac{1}{2i\pi} \int_\gamma e^{\lambda n} G_\lambda(l, j) d\lambda,$$

where  $\gamma$  is at first a path lying in  $\{\Re(\lambda) > 0\}$ . But, thanks to the extension of  $\lambda \mapsto G_\lambda(\cdot; l)$  and the Cauchy formula, we are able to choose paths of integration that may cross the imaginary axis. One must be very careful with the value  $\lambda = 0$  that can be a pole of  $\lambda \mapsto G_\lambda$ : a stationary residue may appear.

Estimates for the boundary layer problem can be obtained with the same techniques : they are a crucial step towards the proof of the convergence of the scheme when large boundary layers occur, as was done in the viscous setting by Grenier and Rousset [4]. The convergence in the discrete case with small amplitude boundary layers was proved by Chainais-Hillairet and Grenier [1].

## References

- [1] C. Chainais-Hillairet and E. Grenier. Numerical boundary layers for hyperbolic systems in 1-D. *M2AN Math. Model. Numer. Anal.*, 35(1):91–106, 2001.
- [2] R. A. Gardner and K. Zumbrun. The gap lemma and geometric criteria for instability of viscous shock profiles. *Comm. Pure Appl. Math.*, 51(7):797–855, 1998.
- [3] P. Godillon. Green's function pointwise estimates for the modified Lax-Friedrichs scheme. *Submitted*, 2001.
- [4] E. Grenier and F. Rousset. Stability of one-dimensional boundary layers by using Green's functions. *Comm. Pure Appl. Math.*, 54(11):1343–1385, 2001.
- [5] K. Zumbrun and P. Howard. Pointwise semigroup methods and stability of viscous shock waves. *Indiana Univ. Math. J.*, 47(3):741–871, 1998.

#### 4.14 Tuesday, Session 1 (afternoon): Adaptive methods II

##### Computational Design of the Adaptive Vertical Coordinate Ocean Circulation Model

Tony Song

*Jet Propulsion Laboratory, California Institute of Technology, Oak Grove Drive, Pasadena, CA*

An adaptive vertical coordinate system is introduced to better represent the sub gridscale mixing and bottom boundary layer processes in numerical ocean models. The new vertical coordinate system is formulated by combining three techniques: arbitrary vertical coordinate system of Kasahara (1974), the general pressure gradient formulation of Song (1998) and a new buoyant parameter which permits a smooth transition scheme to represent the optimal features of commonly-used  $z$ ,  $\sigma$  and  $\rho$  coordinates. The numerical design is based on a staggered finite volume method to ensure conservation of physical properties without altering numerical accuracy in the cases of arbitrary distorted volumes and can be easily applied to any existing ocean model. Three different problems: a coastal canyon, a basin scale circulation and a global ocean circulation are used to demonstrate the capability of the new model formulation for a hierarchy of scales from coastal to global. Our modeling results based on the S-Coordinate Rutgers University Model (Song and Haidvogel 1994) show that the new model is capable of simultaneously simulating both shallow and deep ocean processes without incurring computational expense. The applications show that the adaptive feature allows diverse modelers to chose desired vertical structure for a wide range of geophysical flow problems and to share modeling resources in a uniformed numerical formulation.

##### Three dimensional numerical modelling convective instability by supernova expolsion with nested grids scheme on multiprocessors systems

Sergey D. Ustyugov\* and Alexander N. Andrianov

*Keldysh Institute of Applied Mathematics, Russia*

We carried out three dimensional hydrodynamical simulations to study development large scale convective instability into a protoneutron star by supernova expolsion II type. The initial state is rotating protoneutron star with excess entropy at the centre. On the last stage of collapse of the iron core of a star the process of nonequilibrium neutronization of matter provides high entropy and great mean energy of the neutrinos in the central part of the protoneutron star. The hydrodynamically unstable configuration of a protoneutron star is formed. The statement of the problem consists in studing the development of the nonuniformity scale of the entropy distribution. The central density and central temperature was taken to be  $\rho = 10^{14} \text{g/cm}^3$  and  $T = 10^{11} \text{K}$ . On the boundary of numerical region we keep initial equilibrium values of all variables. The weak solid-body rotation of protoneutron star was taken into account, with the ratio of the rotational kinetic energy  $T$  to the gravitational energy  $|W|$  being  $T/|W| = 0.01$ . The coordinate system was chosen so that the plane of rotation of the star coincided with the  $xy$  plane. It was assumed that relativistic degenerate electrons and an ideal nonrelativistic Fermi gas of nucleons contribute to the equation of a state of substance inside the star. The excess entropy was produced close to the center of the star and had functional form  $S = S_0 + (S' - S_0) \exp\{-|\vec{r} - \vec{r}_0|/|b|\}$ ,  $S' = 3S_0$  and  $r_0 = 0$ . The equations of hydrodynamics, in the adiabatic approximation  $dS/dt = 0$ , with gravitation was used to model the convective processes. In the adiabatic formulation, the entropy shows the evolution of the dredge-up of hot, lighter matter. The hydrodynamic equations was written in conservative form

$$\frac{\partial \vec{U}}{\partial t} + \frac{\partial \vec{F}}{\partial x} + \frac{\partial \vec{G}}{\partial y} + \frac{\partial \vec{H}}{\partial z} = \vec{S}$$

The numerical method which we used was an explicit Godunov-type conservative TVD difference scheme with second order by space and time

$$U_{i,j,k}^{n+1} = U_{i,j,k}^n - \Delta t L(U_{i,j,k}^n),$$

where  $\Delta t = t^{n+1} - t^n$  and  $L$  is

$$L(U_{i,j,k}) = \frac{\tilde{F}_{i+1/2,j,k} - \tilde{F}_{i-1/2,j,k}}{\Delta x_i} + \frac{\tilde{G}_{i,j+1/2,k} - \tilde{G}_{i,j-1/2,k}}{\Delta y_j} + \frac{\tilde{H}_{i,j,k+1/2} - \tilde{H}_{i,j,k-1/2}}{\Delta z_k} + S_{i,j,k}$$

Fluxes along each direction, for example x, was defined by local-characteristic method [1] as follows

$$\tilde{F}_{i+1/2,j,k} = \frac{1}{2} [F_{i,j,k} + F_{i+1,j,k} + R_{i+1/2} W_{i+1/2}]$$

where  $R_{i+1/2}$  is matrix right eigenvectors of Jacobian matrix  $A(U) = \partial F / \partial U$ .

The elements  $l$  of vectors  $W_{i+1/2}$  is

$$(\phi_{i+1/2}^l)^U = \frac{1}{2} \psi(a_{i+1/2}^l) (g_{i+1}^l + g_i^l) - \psi(a_{i+1/2}^l + \gamma_{i+1/2}^l) \alpha_{i+1/2}^l$$

where

$$\gamma_{i+1/2}^l = \frac{1}{2} \psi(a_{i+1/2}^l) \begin{cases} (g_{i+1}^l - g_i^l) / \alpha_{i+1/2}^l & , \alpha_{i+1/2}^l \neq 0 \\ 0 & , \alpha_{i+1/2}^l = 0 \end{cases}$$

The amplitude of waves  $\alpha_{i+1/2}^l$  is elements of vectors

$$\alpha_{i+1/2} = R_{i+1/2}^{-1} (U_{i+1,j,k} - U_{i,j,k}).$$

The function  $\psi$  is

$$\psi(z) = \begin{cases} |z| & , |z| \geq \delta_1 \\ (z^2 + \delta_1^2) / 2\delta_1 & , |z| < \delta_1 \end{cases}$$

and define entropy correction by  $|z|$ , where  $\delta_1$ -small positive parameter. The function-limiter  $g_i^l$  was defined as follows:

$$g_i^l = \minmod(\alpha_{i-1/2}^l, \alpha_{i+1/2}^l)$$

$$g_i^l = (\alpha_{i+1/2}^l \alpha_{i-1/2}^l + |\alpha_{i+1/2}^l \alpha_{i-1/2}^l|) / (\alpha_{i+1/2}^l + \alpha_{i-1/2}^l)$$

The one step of time integration is defined by Runge-Kutta method [2] as

$$\begin{aligned} U^{(1)} &= U^n + \Delta t L(U^n) \\ U^{(2)} &= \frac{3}{4} U^n + \frac{1}{4} U^{(1)} + \frac{1}{4} \Delta t L(U^{(1)}) \\ U^{n+1} &= \frac{1}{3} U^n + \frac{2}{3} U^{(2)} + \frac{2}{3} \Delta t L(U^{(2)}) \end{aligned}$$

The time step is restricted to satisfy the Courant condition along each row in three directions, and is calculated with

$$\Delta t = CFL \times \min \left( \frac{\Delta x}{|v_x| + c_s}, \frac{\Delta y}{|v_y| + c_s}, \frac{\Delta z}{|v_z| + c_s} \right)$$

and  $CFL = 0.2$  typically.  $v_x, v_y, v_z$  are the velocity of matter in each direction and  $c_s$  is the speed of sound.

For higher resolution in the numerical modelling we have used three level of nested rectangular grids with 128 cells in each directions. Solution results for above described problem were obtained due to the NORMA system application [3] on the system with distributed memory multiprocesseres ( two Alpha 21264/667 MHz in node, memory 1 Gb in node, SAN Myrinet